

AD-A228 920

AFOSR-TR-90-1153  
BTIC FILE COPY ②

AFW / M-B / 90-1

**EFFECTS OF FREE STREAM TURBULENCE  
ON HEAT TRANSFER**

FINAL REPORT  
AFOSR F49620-87-k-0008 P0004

April 1, 1987 through July 31, 1990

Dated: September 27, 1990

Based on Research Performed At  
Purdue University and Imperial College, London

Prepared By

S.N.B. Murthy  
School of Mechanical Engineering  
Purdue University  
W. Lafayette, IN 47907

and

P. Bradshaw  
Department of Mechanical Engineering  
Stanford University  
Stanford, CA 94305

Approved  
[Signature]

**DTIC**  
**ELECTE**  
**NOV 19 1990**  
**S E D**

90 11 19 215

## REPORT DOCUMENTATION PAGE

1a. REPORT SECURITY CLASSIFICATION <b>UNCLASSIFIED</b>			1b. RESTRICTIVE MARKINGS none		
2a. SECURITY CLASSIFICATION AUTHORITY			3. DISTRIBUTION/AVAILABILITY OF REPORT <b>APPROVED FOR PUBLIC RELEASE DISTRIBUTION IS UNLIMITED</b>		
2b. DECLASSIFICATION/DOWNGRADING SCHEDULE			4. PERFORMING ORGANIZATION REPORT NUMBER(S) AFW / M-B/ 90-1		
4. PERFORMING ORGANIZATION REPORT NUMBER(S) AFW / M-B/ 90-1			5. MONITORING ORGANIZATION REPORT NUMBER(S)		
6a. NAME OF PERFORMING ORGANIZATION Purdue University and Imperial College, London		6b. OFFICE SYMBOL (if applicable) -	7a. NAME OF MONITORING ORGANIZATION AFOSR/NA		
6c. ADDRESS (City, State, and ZIP Code)			7b. ADDRESS (City, State, and ZIP Code) BUILDING 410 BOLLING AFB, DC 20332-6448		
8a. NAME OF FUNDING/SPONSORING ORGANIZATION AFOSR		8b. OFFICE SYMBOL (if applicable) NA	9. PROCUREMENT INSTRUMENT IDENTIFICATION NUMBER <b>F49620-87-K-0008</b>		
8c. ADDRESS (City, State, and ZIP Code) BUILDING 410 BOLLING AFB, DC 20332-6448			10. SOURCE OF FUNDING NUMBERS	PROGRAM ELEMENT NO. 61102F	PROJECT NO. 2307
				TASK NO. A46	WORK UNIT ACCESSION NO.
11. TITLE (Include Security Classification) Influence of <u>Free Stream Turbulence</u> on Heat Transfer (Unclassified)					
12. PERSONAL AUTHOR(S) S.N.B. Murthy and P. Bradshaw					
13a. TYPE OF REPORT Final		13b. TIME COVERED FROM 87 04 01 TO 90 07 31		14. DATE OF REPORT (Year, Month, Day) 90 09 28	15. PAGE COUNT 92 = (iv) + 88
16. SUPPLEMENTARY NOTATION <b>Boundary layer turbulence (BLT)</b>					
17. COSATI CODES			18. SUBJECT TERMS (Continue on reverse if necessary and identify by block number)		
FIELD	GROUP	SUB-GROUP	Free Stream Turbulence; Boundary Layer; Heat Transfer; Inhomogeneous Turbulence; Turbines		
19. ABSTRACT (Continue on reverse if necessary and identify by block number) → The Report presents the research (including relevant publications) undertaken at Purdue University and, under subcontract, at Imperial College, London, on analytical-computational and experimental studies on the determination of the influence of inhomogeneous and isotropic turbulence on boundary layers, including cases with heat transfer. The modelling of the influence of <del>FST</del> on <del>BLT</del> has been based on the so-called large eddy interaction hypothesis, wherein the interaction between a representative large eddy and all of the eddies is related to a skewness factor and a damping factor. The boundary layer is divided into four asymptotically matched regions, including the free stream, and the flowfield is calculated based on the necessary (as proved herein) assumption of the existence of a logarithmic law region adjoining the wall viscous region. A detailed comparison between the experimental data of P.E. Hancock and P. Bradshaw and the predictions obtained for the same case of interaction between FST and BLT is a fully-developed TBL is presented and provides substantial credibility to the method of approach. The experimental work at → <b>OVER</b> Continued on (ii)					
20. DISTRIBUTION/AVAILABILITY OF ABSTRACT <input type="checkbox"/> UNCLASSIFIED/UNLIMITED <input checked="" type="checkbox"/> SAME AS RPT. <input type="checkbox"/> DTIC USERS			21. ABSTRACT SECURITY CLASSIFICATION UNCLASSIFIED		
22a. NAME OF RESPONSIBLE INDIVIDUAL JAMES M. McMICHAEL			22b. TELEPHONE (Include Area Code) 202-767-4936	22c. OFFICE SYMBOL AFOSR/NA	

## 19. Abstract (cont'd)

Imperial College has been devoted to a study of the effects of anisotropic FST on heat transfer in low speed TBL. The experiments and the results obtained in three stages, first, with isotropic turbulence, second, with turbulence generated with oscillating spanwise rods and third, on turbulence generated with the wake of a stationary rod slightly inclined to the spanwise direction, are described. Stage three investigations pertain to simulation of non-radial blading in turbomachinery. The main findings are (i) the difficulty of establishing a simple correlation parameter for heat transfer even with isotropic turbulence accounting for turbulence intensity and scale; (ii) the specific nature of FST in various experimental studies that prevents comparison of results; and (iii) the rather small influence of non-radial nature of turbine blades on the wakes generated by them. A considerable body of experimental data, including correlations and spectra, have been obtained in various cases.

## PREFACE

The Final Report presents the main objectives and accomplishments of the project. Following the Introduction, in Part I, the research undertaken at Purdue University on analytical-computational studies is presented along with relevant publications. In Part II, the research undertaken at Imperial College, London, on experimental studies conducted to establish various aspects of the influence of free stream turbulence (isotropic and nonisotropic) on low speed, fully developed, turbulent boundary layer is presented along with relevant publications. An addendum to the Final Report includes two appendices, one on the large eddy interaction hypothesis and the other on structural similarity between velocity and temperature fields.



Accession For	
NTIS GRA&I	<input checked="" type="checkbox"/>
DTIC TAB	<input type="checkbox"/>
Unannounced	<input type="checkbox"/>
Justification	
By _____	
Distribution/	
Availability Codes	
Dist	Avail and/or Special
A-1	

## TABLE OF CONTENTS

	page
1. Introduction	
1.1 Objectives of the Investigation.....	2
1.2 Main Accomplishments.....	3
1.3 Outline of Report.....	5
 <u>Part I</u>	
I.1. Large Eddy Interaction Hypothesis.....	9
I.2. Boundary Layer Predictions with Free Stream Turbulence...	10
I.2.1. Physical Structural Features.....	12
I.2.2. Boundary Layer Predictions.....	14
I.3. Structural Similarity Between Velocity and Temperature.....	14
I.3.1. Experimental Studies on Velocity and Temperature Fluctuations.....	18
I.3.2. Modelling of Temperature Fluctuations.....	18
I.3.3. Spectra.....	22
I.3.4. Correlations in the Wall Region.....	23
I.3.5. Spectra in the Logarithmic Region.....	24
I.4. Prospects for Future Investigations.....	24
* References	
* Copies of Relevant Publications	
 <u>Part II</u>	
II.1. Introduction.....	II.1
II.2. Equipment and Techniques.....	II.2
II.3. Results.....	II.2
II.3.1. First Stage - Isotropic Free Stream Turbulence.....	II.2
II.3.2. Second Stage - Wakes of Spanwise Rods.....	II.2
II.3.3. Third Stage - Wake of a Stationary Inclined Rod....	II.3
II.4. Conclusions.....	II.4
* Copies of Relevant Publications	

## 1. INTRODUCTION

The general problem of interaction between two distinguishable fluid flows is of fundamental interest and also of common occurrence in nature and engineering. The problem becomes considerably complex when one of the flows is vortical or turbulent even when both flows are incompressible. The presence of free stream turbulence in a wall-bounded flow provides an example of such a complex flow. It can be expected to affect both skin friction as well as heat transfer, and also transition in the boundary layer when otherwise the boundary layer may have remained laminar. The physical processes involved in such interactions are not fully understood and, therefore, prediction schemes have remained generally ad hoc even for the simplest type of interactions.

The effects of free stream turbulence are of interest in several internal and external flows in engines and flight vehicles. Those flows involve additional complications such as pressure gradient, wall geometry and various means of cooling, for instance film cooling. Also, there can be complexities in the nature of free stream turbulence, inhomogeneity in the large scales of turbulence being a common occurrence in combustion devices and atmospheric flows.

A body of literature representing the current state of knowledge in the subject area can be found in Refs. 1 - 12. In general it is found that there has been no systematic study of the effects of inhomogeneity in free stream turbulence. An interesting study in this connection is reported in Ref. 13 on peaky turbulence.

In the study of interaction of turbulence flowfields, such as free stream turbulence (FST) and boundary layer turbulence (BLT), the physical processes may be fully understood only by an appeal to a combination of the classical structure as depicted by statistical, point-wise information and the more modern, quasi-deterministic, physical structure. Data sets available on classical structure are not always without ambiguity and in no case include pressure fluctuations in the flowfield. There are no flow

visualization or quantitative data on physical structures in a boundary layer with heat transfer or free stream turbulence.

It may be worth pointing out that pressure fluctuations are of interest in turbulent flow interactions even under the conditions of incompressible flow. Unfortunately there are no data sets that relate free stream pressure fluctuations with even wall surface pressure fluctuations. The main difficulties are two-fold: (i) obtaining pressure fluctuation-data with spectral information included and (ii) extent of data required in order to relate time-dependent variation of pressure to (a) the velocity scales of interest otherwise and (b) the dynamics of turbulence production adjacent to the boundary wall (Ref. 12).

In analytical-computational studies, understanding in terms of physical structures and their dynamics may become feasible as there comes about further progress in large eddy simulation or solution of Navier-Stokes equations (without time-averaging) and the needed computational capability. On the other hand,, one can try to obtain the best out of classical description of turbulence. A significant proposal in this regard is John Lumley's so-called rational description of turbulence (Ref. 14, 15). It is interesting that turbulence models that can be generated from it have been utilized to extract physical structural details in various contexts (Refs. 16-19). Predictive tools may also be developed based on that description of turbulence. This is the basis of the analytical computational work undertaken in the current project.

### 1.1 Objectives of the Investigation

The original objectives included both experimental (at Imperial College, London) and analytical-computational studies (at Purdue University).

The flowfield considered was a simple one: incompressible flow past a flat plate under conditions of heat transfer, with no external pressure gradient, when the boundary layer is fully turbulent and the free stream is turbulent and homogeneous or with a few dominant large scales in it.

The objectives in the experimental studies were to obtain measurements of turbulence quantities and their structure in the classical sense. In the analytical-computational studies, it was proposed to adopt the classical, statistical description again. However, turbulence was sought to be modelled on the basis of John Lumley's rational description of turbulence and its adaptation at Purdue University in the form of what has come to be called the large eddy interaction hypothesis (Refs. 20-24). The modelling was to be developed for obtaining both the momentum and stress distributions and the heat transport while the illustrative calculations did not include the latter.

## 1.2 Main Accomplishments

### 1.2.1. Publications

1. S.N.B. Murthy and S.K. Hong: Turbulence Boundary Layer with Free Stream Turbulence, AIAA 90-1503, AIAA 21st Fluid Dynamics, Plasma Dynamics and Lasers Conference, June 1990. (Attached at the end of Part I of this Report).
2. V. Bhaskaran, O.E. Abdellatif and P. Bradshaw: Effects of Free Stream Turbulence on Turbulent Boundary Layers with Convective Heat Transfer, Seventh Symposium on Turbulence Shear Flows, Stanford University, August 1989. (Attached at the end of Part II of this Report).
3. V. Bhaskaran and P. Bradshaw: An Experimental Study into the Wake-Boundary Layer Transition, 10th Australian Fluid Mechanics Conference, December 1989. (Attached at the end of Part II of this Report).
4. S.N.B. Murthy: Turbulence-Mean Discontinuity in Supersonic Flow, Meeting on the Physics of Compressible Turbulent Mixing, Princeton University, Princeton NJ, October 1988. (Attached at the end of Part I of this Report).

### 1.2.2. Scientific Advances

1. *Application of large eddy interaction hypothesis:* A four-layer boundary layer model has been developed, along with a numerical code for prediction of the flowfield, for an incompressible, zero-pressure gradient, fully turbulent boundary layer with moderate levels and scales of (grid-generated) free stream turbulence. The Hancock-Bradshaw measurements at Imperial College have been reproduced in most parts utilizing a skewness and a damping factor. A converged solution can be obtained in 400-600 iterations.

2. *Logarithmic region of boundary layer:* The numerical work described in item 1 provides the basis for a conclusion that a boundary layer type solution in the presence of free stream turbulence requires necessarily a region with mean flow governed by the so-called log law. In the current predictions it has been essential to assume the existence of a layer governed by log law; the extent of that region, of course, is a part of the solution. In other words, the presence of free stream turbulence permits a variety of mean flow profiles, when only initial and boundary conditions are specified, and the physical flow can then be selected only on specifying the existence of a region governed by log law.

3. *Skin friction in a turbulent boundary layer:* In the experimental studies, it has been found that the skin friction in a turbulent boundary layer on a flat plate decreases in the presence of the wake of an upstream mounted cylinder representing an axial turbomachine blade, in contrast to the increase in  $C_f$  produced by multiple-rod grids. Evidently the primary effect is the reduction in "free stream" velocity seen by the boundary layer, as a consequence of the velocity defect in the cylinder wake: interaction between the turbulence fields of the wake and the boundary layer are less important. The details of the flow, particularly in the present case where the cylinder axis is inclined to the plane of the boundary layer, are of considerably interest.

4. *Skin friction coefficient and Stanton number:* From experimental studies, it is found that skin friction coefficients and Stanton numbers were measured in a flat plate boundary layer beneath grid-generated free stream turbulence, with a maximum rms intensity of 8 percent of the free stream velocity and a maximum length scale of 6 times the local boundary layer thickness. The increase in skin friction coefficient agrees well with the correlation curve based on the variable,  $\sqrt{u_{\tau}^2} / U_{\infty}(L/\delta+2)$ , proposed by Hancock & Bradshaw (1983). Stanton number increases do not seem to follow the proposed skin friction correlation or any simple multiple of it, indicating that the Reynolds analogy factor is changing significantly - more than in the work of Blair (1983). A change in the above empirical variable to improve Stanton number predictions is tentatively suggested.

5. *Influence of moving rod arrays:* The wake of a spanwise rod mounted ahead of the test plate to simulate turbomachine blade wakes produced a *reduction* in skin friction, calling into question the interpretation of published results from moving rod arrays.

### 1.3 Outline of Report

The report is divided into two parts. Part I presents the work undertaken at Purdue University. Section 2 deals with turbulent boundary layer-free stream turbulence interactions. The method of calculating a flowfield utilizing LEIH is illustrated in the attached publications, wherein the flowfield measured by Hancock and Bradshaw (Refs. 25-26) has been chosen for prediction. Section 3 then deals with the possibility of invoking classical structural similarity between turbulence intensity and temperature variance in different forms across a boundary layer during heat transfer.

The conclusions from the overall effort and the type of extensions that appear significant are discussed in Section 4.

Part II deals with the effort accomplished at the Imperial College of Science, Technology and Medicine, London, U.K., under a subcontract for experimental studies in the subject. This part consists of the report received from Professor Peter Bradshaw, the Principal Investigator for the project at Imperial College.

PART I

SUMMARY OF PURDUE UNIVERSITY WORK  
ON FREE STREAM TURBULENCE  
AND  
HEAT TRANSFER

S.N.B. MURTHY

TABLE OF CONTENTS

	page
I.1. Large Eddy Interaction Hypothesis.....	9
I.2. Boundary Layer Predictions with Free Stream Turbulence....	10
I.2.1. Physical Structural Features.....	12
I.2.2. Boundary Layer Predictions.....	14
I.3. Structural Similarity Between Velocity and Temperature.....	14
I.3.1. Experimental Studies on Velocity and Temperature Fluctuations.....	18
I.3.2. Modelling of Temperature Fluctuations.....	18
I.3.3. Spectra.....	22
I.3.4. Correlations in the Near-Wall Region.....	23
I.3.5. Spectra in the Logarithmic Law Region.....	24
I.4. Prospects for Future Investigations.....	24
* Appendix I. Background on Large Eddy Interaction Hypothesis.	
* Appendix II. Background on Structural Similarity Between Velocity and Temperature.	
* Copies of Relevant Publications.	

## I.1. LARGE EDDY INTERACTION HYPOTHESIS

The general background to the development of the hypothesis, LEIH, is provided in Appendix I.

A number of features of the hypothesis and its application to boundary layer problems are also presented therein.

## I.2. BOUNDARY LAYER PREDICTIONS WITH FREE STREAM TURBULENCE

The asymptotic matching of the boundary layer regions with the free stream has been discussed by T. Tennekes (Ref. 27), K.S. Yagnik (Ref. 28) and G.L. Mellor (Ref. 29), in all cases in the absence of turbulence in the free stream. The objective has been to establish the connections between the so-called inner, viscous layer, the outer layer and the free stream. Various types of assumptions are introduced in the course of asymptotic analysis and matching of layers. For example, a key assumption of the case of G.L. Mellor is that the Reynolds stress is of the same order of magnitude in the inner and the outer layers.

An important conclusion of G.L. Mellor, then, is that the outer Reynolds stress asymptote of viscous region (the inner layer) must behave just the same as the inner Reynolds stress asymptotic of the defect region (the outer layer). In fact, therefore, the asymptotic analysis provides a basis for a region governed by the log-law, which was rationalized by F. Clausen, based on the postulates of L. Prandtl and von Karman, namely the velocity distribution and the reduction in velocity from that of the free stream must both be functions of wall shear, distance from the surface and fluid kinematic viscosity in the first case and overall thickness of boundary layer in the second.

On including free stream turbulence, several considerations arise on amount of the intensity and the length scale of such turbulence. Both intensity and length scale vary along the flow depending upon the manner in which the free stream turbulence is generated.

Returning to the problem of asymptotic matching the free stream velocities, Reynolds stresses and coordinates may again be nondimensionalized based on a velocity  $u_0$ , a characteristic turbulence velocity  $u_i$  (which may be the same as  $u_\tau$ , the friction velocity) and a length scale  $l$ .

Two small parameters that appear in the describing equations for the boundary region are the following.

$$\varepsilon \equiv \frac{u_i}{u_o} \quad \text{and} \quad \varepsilon^2 \hat{\varepsilon} \equiv \frac{\nu}{u_o \ell},$$

where  $\nu$  is the kinematic viscosity. G.L. Mellor then introduces a length scale for the defect region, namely

$$\Delta_\ell \equiv \varepsilon \ell. \quad (2.1)$$

It may also be noted here that  $\varepsilon$  and  $\hat{\varepsilon}$  are in the nature of ratios of (length scales) in the viscous, the defect and the free stream layers. With free stream turbulence of a given scale  $\ell_f$  one can construct a length scale for the free stream layer that becomes coupled to the boundary layer, namely

$$\Delta_f \equiv \varepsilon^* \ell_f, \quad (2.2)$$

where  $\varepsilon^*$  is given by

$$\varepsilon^* \equiv \frac{u_f}{u_\ell} \quad (2.3)$$

with  $u_f \equiv 1/3 \cdot u_{fij}^2$ , the representative turbulence velocity of the free stream.

It is then necessary to distinguish between the following cases:

- (i)  $\Delta_f \ll \Delta_\ell$ ,
- (ii)  $\Delta_f \approx \Delta_\ell$ , and
- (iii)  $\Delta_f \gg \Delta_\ell$ .

The case of immediate interest is (ii) in which the free stream turbulence scale is comparable to the boundary layer scale. It is felt that, while in case (i) the interaction between the free stream and the boundary layer is minimal, case (iii) may require a completely different approach.

In case (ii), a model can be set up with four layers: (i) the unaffected free stream, (ii) the free stream layer affected by interaction, (iii) the defect layer and (iv) the viscous layer. Now, when asymptotic matching of the layers is carried out, it is found that

(a) the inner asymptote of the defect layer and the outer asymptote of the viscous layer again become identical; and

(b) the magnitude of the Reynolds stresses in the viscous layer becomes modified on account of the Reynolds stresses of the free stream affecting the defect layer.

Result (a) is of great significance because it shows why a region of log law character persists even with free stream turbulence. Thus, in all cases, it appears that a viscous layer at the wall may be matched with the defect layer only through the presence of a log law layer. Furthermore, as Reynolds number and  $u_\tau$  increase, the extent of the log law region grows with a corresponding (relative) reduction of the outer part of the defect layer. In fact, the "defect" spreads into the free stream.

There are several implications of the foregoing, which will be discussed.

### 1.2.1. Physical Structural Features

Based on the currently well-accepted descriptions of the physical structure of boundary layers in terms of periodic bursts and unstable hairpin vortices, the influence of free stream turbulence can be described in terms of the following.

(i) The perturbed spanwise vortex, which results in a hairpin vortex with its dynamical features, also interacts with the vorticity of free stream turbulence. And,

(ii) The results is a modification in the magnitude and distribution of Reynolds stresses without a modification of the character of interactions.

No attempt has been made to-date on obtaining the modification to the essential physical structure of a boundary layer subjected to externally imposed vorticity, particularly fluctuating vorticity.

Writing the overall stress tensor in the form, namely

$$T_{ij} = -P \delta_{ij} + 2 \mu S_{ij} = \zeta \overline{u_i u_j}, \quad (2.4)$$

one can write the momentum, energy and vorticity equations as follows.

$$U_j U_{i,j} = (T_{ij} / \zeta), j \quad (2.5)$$

$$\rho U_j \left( \frac{1}{2} U_i U_j \right), j = (T_{ij} U_j), j \quad (2.6)$$

$$U_j (\Omega_i), j = - \overline{u_j \omega_{i,j}} + \overline{\omega_j s_{ij}} + \Omega_j S_{ij} + \nu \Omega_{,ij} \quad (2.7)$$

The mean vorticity equation shows the combined effect of fluctuations of vorticity and strain. Whether additional mean or fluctuating vorticity and additional strain can give rise to entirely new turbulent processes is not clear. However, currently available data indicate a change in the shear stress and the outer intermittency that do not require any new processes other than those currently accepted in a boundary layer.

### 1.2.2. Boundary Layer Predictions

In the context of LEIH, it is necessary to model eddy-eddy interactions, for example in terms of the skewness and the eddy viscosity factors. In predicting the (classical) structure of a boundary conditions, the question arises as to the selection of the two aforementioned factors. The most rational basis for the selection of the two factors, then, appears to be that the selected values of the two factors must yield a region of log law character adjoining the viscous layer, both as a necessary and a sufficient condition.

This has become evident in predictive calculations (reference 30). However the rationalization is based on the results of asymptotic analysis.

### 1.3. STRUCTURAL SIMILARITY BETWEEN VELOCITY AND TEMPERATURE

The vast body of literature on convective heat transfer appeals to the possible analogy between heat and momentum transport, in terms of the Prandtl number, based on the so-called Reynolds analogy, to determine heat transfer to a boundary wall in the fluid. In turbulent flow this is equivalent to drawing an analogy between eddy diffusivities of heat and momentum. In mixing length theory, a ratio of mixing lengths for heat and momentum is implied. The eddy diffusivity for heat may be defined by

$$\gamma_T = - \overline{v\theta} / (\partial \overline{T} / \partial y) \quad (3.1)$$

where  $\theta$  is the fluctuating temperature. The turbulent Prandtl number is then given by

$$Pr_T = c_p \mu_t / \gamma_T \quad (3.2)$$

where  $c_p$  is the specific heat at constant pressure. The turbulent Prandtl number is assumed to be constant across the boundary layer, defined by

$$\sigma_T = [\overline{uv} / (\partial U / \partial y)] / [\overline{v\theta} / (\partial T / \partial y)] \quad (3.3)$$

where

$$U = u_\tau f(yu_\tau / \nu_w, \beta), \quad (3.4)$$

$$T = T_w f(yu_\tau / \nu_w, \beta), \quad (3.5)$$

$\beta$  being equal to  $T_c / T_w$ ;  $T_c$  is Squire's "friction temperature". The functional relationships have been specifically determined for various classes of flows and different parts of a given turbulent boundary layer.

It may be worth noting here that there are limited, often controversial, experimental data and largely, ad hoc theories to determine the influence of molecular Reynolds and Prandtl numbers on  $\sigma_T$ .

Returning to the consideration of different parts of a boundary layer, there is the outer boundary region, the interface that separates the boundary layer and the free stream. The free stream may have additional complexities such as pressure gradient and turbulence. The interface thickness is negligibly small at high Reynolds numbers, but of the order of the sublayer thickness or slightly larger. The pressure fluctuations cause velocity fluctuations over an extent of the adjoining free stream, but there are no vorticity fluctuations in the free stream. However the extent of the region over which temperature fluctuations is felt depends upon the temperature diffusivity. The difference in interface propagation velocity and velocity of entrainment of free stream fluid should also be noted. In heat transfer problems one is primarily interested in the entrainment of outer fluid into the boundary layer. The nature and magnitude of entrainment in the presence of free stream turbulence is a crucial issue; the influence of pressure fluctuations must also be included in any calculations.

The other part of a turbulent boundary layer that needs detailed consideration in heat transfer is the so-called inner layer: the combined extent of the linear sublayer (where viscous stresses are large compared to Reynolds stresses), the buffer layer (where viscous and Reynolds stresses are of the same order of magnitude) and the logarithmic law region (where Reynolds stresses are large compared to viscous stresses). As elsewhere, the logarithmic law region may be distinguished from the sublayer, the latter including the buffer layer which must necessarily be thin. The sublayer is an inhomogeneous region with oscillatory and time-dependent growth of streaks interspersed between quiescent periods. The oscillatory motion is organized in several respects. Insofar as heat flux transport is concerned, it is not clear if there is a basic modification to turbulence structure in the presence of heat transfer in incompressible flows. For instance, one can pose the question of whether there is a difference in heat transfer between the cases of hot fluid and cold boundary and cold fluid and hot boundary.

If one considers the equation for the rate of transport of heat, the mechanisms for limiting the growth of the flux consist of (a) direct dissipation which is small and (b) pressure-temperature gradient correlation. From a structural point of view the influence of pressure fluctuations must depend upon the dynamics of the finite structures in the boundary layer, which, in incompressible flow, cannot depend upon the temperature of the fluid. Of course, the molecular viscosity of the fluid is a function of temperature, but in high Reynolds number flows the change in viscosity is ordinarily not effective in modifying diffusion or dissipation to any appreciable extent.

On the other hand, the entrapment of hot fluid in the spaces between finite structural entities and its dynamics can influence heat transfer directly through the influence of thermal conductivity. It is the influence of such entrapped fluid parcels (some cold and others hot) that brings about a difference between the cases of relatively cold and hot boundary wall. Some aspects of entrapment of fluid are discussed in Ref. 31. However, there is still great uncertainty in the dynamics of the structures; for

instance the time scales associated with the motion of the structures are not established.

Both the outer layer and the inner layer processes, of course, have been studied in the presence of heat transfer through statistical theory of turbulence applied to space-time points. In this case, the primary interest is in the relation between the spectra of velocity and temperature.

In that connection, it is of interest to recall the following:

(i) In Ref. 32, the correlation  $\overline{u_i u_j \theta}$  has been written as a function of  $\overline{q^2} / \epsilon$ ,  $\overline{u_i u_i}$ ,  $\overline{u_i u_j}$  and  $\overline{u_i \theta}$ .

(ii) In Ref. 33,  $\overline{u_i \theta}$  has been modelled as a function of  $\overline{q^2} / \epsilon$ ,  $\overline{u_i u_i}$  and  $\partial T / \partial x_i$ , taking also into account generation of  $1/2 \overline{\theta^2}$  and a time scale ratio for the decay of temperature and velocity fluctuations,  $R \equiv \left[ \left( \overline{\theta^2} / \overline{q^2} \right) \cdot (\epsilon / \epsilon_\theta) \right]$ . And, finally,

(iii) in Ref. 34, the heat flux is modelled in the form

$$-\overline{v\theta} = a_\theta q \sqrt{\overline{\theta^2}} \quad (3.6)$$

where  $a_\theta$  is a dimensionless function of position in the boundary layer. One then needs a balance equation for  $(1/2 \overline{\theta^2})$  which involves a model for the term  $\overline{u_j \theta^2}$ . This is written in the following form.

$$-\overline{u_j \theta^2} \propto \overline{\theta^2} V'_i \quad (3.7)$$

where a so-called bulk convection velocity is introduced, again as a function of position in the boundary layer. It may be pointed out that the resulting equations become hyperbolic and indicate equilibrium near the wall. A critique on this approximation may be found in Ref. 35, p. 125, 267 and 298.

In (ii) of the foregoing, there arises, as pointed out earlier, the time scale ratio  $R$ , which can also be constructed for turbulence intensity in anisotropic flow. It involves the variance of temperature fluctuations and the intensity of turbulence. However, the relation between  $\overline{u_i \theta}$  and  $R$  turns out to be rather involved. On the other hand, considering a similar relation for  $\overline{u_i u_j}$ , one can write

$$\frac{\overline{u_i u_j}}{v \theta} = \frac{a_q}{a_\theta} \cdot \frac{q_2}{\theta^2} \quad (3.8)$$

where  $a_q$  is a dimensionless constant also. Similarly, one can consider two bulk convection velocities, one for turbulence intensity and another for temperature, with two different constants of proportionality in Eq. 3.7. In both cases, the turbulence intensity and temperature variance can be expected to have a relationship to the relevant spectra.

### I.3.1. Experimental Studies on Velocity and Temperature Fluctuations

A summary of experimental studies on velocity and temperature correlations and spectra in thermal boundary layers is presented in Appendix II of this Report.

### I.3.2. Modelling of Temperature Fluctuations

We concentrate attention on an incompressible fluid flow of high Reynolds number, with temperature as a passive contaminant; the fluid is a gas with Prandtl number approximately equal to unity. The mean heat flux per unit area and per unit time may then be written as follows.

$$Q_j = \rho c_p \left( \overline{\theta u_j} - \gamma \frac{\partial T}{\partial x_j} \right) \quad (3.8)$$

which includes heat flux due to mean temperature gradient and that due to turbulent transport.

Introducing assumptions on the existence of a single length scale and a single temperature scale, one can write the following:

$$\theta' \approx \ell \partial T / \partial \chi_2 \quad (3.9)$$

where  $\theta'$  is the rms value of  $\theta$ . Turbulent heat transfer may then be written as

$$H_2 = -\rho c_p C_5 u_2' \ell \partial T / \partial \chi_2, C_5 \approx 0(1) \quad (3.10)$$

The justification for introducing a mixing length,  $\ell$  is that, while momentum transfer is definitely not merely kinematical and depends upon the dynamics of turbulence, heat transfer perhaps involves only a transport.

Considering the dynamics of temperature fluctuations for the case, again, involving one temperature and one length scale, it can be argued that

$$\overline{\theta u_j} \frac{\partial T}{\partial \chi_j} \approx \overline{\theta^2} \frac{u}{\ell} \quad (3.11)$$

In other words, spectral transfer of temperature fluctuations towards the small dissipative scales occurs at a rate governed by the characteristic time of large eddies and the amount of  $\theta^2$  involved.

It was also shown by S. Corrsin (Ref. 36) that when the molecular Prandtl number is near unity, the following can be deduced.

$$\eta_\theta / \eta (\gamma/\nu)^{1/2} = 1 \quad (3.12)$$

under certain postulates. Thus when  $\gamma \approx \nu$ , temperature fluctuations extend all the way up to  $\eta$ , the Kolmogoroff scale for velocity fluctuation. Molecular transport of heat is accelerated by straining motion in turbulent

flows, although mainly at small scales. Mean temperature distribution is strongly affected by turbulence while it is affected comparatively little by molecular diffusion.

Finally, it is useful to consider the spectrum of temperature variance. The three-dimensional spectrum can be defined as follows

$$E_{\theta}(\mathbf{K}) = \iint \frac{1}{2} \phi_{\theta} d\sigma \quad (3.13)$$

$$\frac{1}{2} \overline{\phi^2} = \int_0^{\omega} E_{\theta}(\mathbf{K}) dK \quad (3.14)$$

It represents the spectral density of waves which have the wave number of magnitude  $K$  regardless of direction and is also the spectrum of temperature variance. It may be pointed out that  $\phi_{\theta}(\mathbf{K})$  is the spatial spectrum being the Fourier transform of the spatial autocorrelation  $R_{\theta}(\mathbf{r})$ .

$$R_{\theta}(\mathbf{r}) = \iiint_{-\infty}^{\infty} \exp(\mathbf{K} \cdot \mathbf{r}) \exp(-\mathbf{K} \cdot \mathbf{r}) \phi_{\theta}(\mathbf{K}) d\mathbf{K} \quad (3.15)$$

$$\phi_{\theta}(\mathbf{K}) = \frac{1}{(2\pi)^3} \iiint_{-\infty}^{\infty} \exp(-i\mathbf{K} \cdot \mathbf{r}) R_{\theta}(\mathbf{r}) d\mathbf{r} \quad (3.16)$$

As in the case of turbulence kinetic energy, one can describe a cascade in temperature spectrum. It is noted that spectral flux of temperature variance is the spectral equivalent of the following:  $u \ell (\partial T / \partial \chi_2)^2$ , where

$$u = [K_2 E(K_2)]^{1/2}$$

$$\ell = 1/K_2.$$

The latter pertains to the smaller eddies that distort the larger eddies. The spectral flux of temperature variance can then be expressed by

$$T_{\theta}(K) = CK^2 E_{\theta}(KE)^{1/2} \quad (3.17)$$

In the foregoing, the temperature gradient associated with an eddy of wave number  $K_1$  is approximated as  $\approx 0 [K_1^3 K_\theta (K_1)]^{1/2}$ . It is also useful to point out that the dissipation of temperature variance may be defined by

$$\eta \equiv \gamma \frac{\overline{\partial\theta}}{\partial\chi_i} \frac{\overline{\partial\theta}}{\partial\chi_j} \quad (3.18)$$

It can be seen from the foregoing that the spectral features of temperature fluctuations depend upon the spectral features of velocity fluctuations, kinematic viscosity, diffusivity of heat, Kolmogoroff scale in the flow, dissipation and the inhomogeneities in the mean strain in the flow.

In the context of applying the LEIH to heat transfer problems, it can be observed that it is most rational and also most convenient if the spectral features of velocity and temperature can be related in anyway. One then does not need to introduce any assumptions, for example, regarding the variation of Prandtl number across a shear layer, which is essentially a ratio of scales.

The question being raised in the context of the use of the LEIH is whether it is not more satisfactory to examine any analogy that may exist in the spectra of velocity and temperature. Several points of significance may be noted here. First, we referred earlier to the cascading of temperature variance; Eq. 3.17 provides the spectral flux of temperature variance. Second, it has been argued that temperature fluctuations are in a sense transported by the total velocity. Temperature fluctuations are related to heat transfer, an "external" process. Thus they correspond to entropy fluctuations. (It is possible to extend the argument to the vorticity fluctuations inherent to turbulence, but does not seem to have been pursued). Third, the effect of molecular diffusion is felt only at the small scales. Finally, while the temperature fluctuation is correlated well with both  $u_1$  and  $u_2$  the Taylor spectra of  $u_1$  and  $\theta$  are different. In this connection, one may also note that close to a wall, the intensities of velocity fluctuations are different, while they are of the same order of magnitude elsewhere in the boundary layer. The difference in spectra of  $u_1$  and  $\theta$  is

in the wave number range contributing most to the variance of the two quantities. At high wave numbers, an analogy can be set up between the two spectra. On the other hand, at low wave numbers, where one does observe a difference, there is obvious interest in the context of using the LEIH.

A series of investigations undertaken by L. Fulachier, R. Dumas, R. Antonia, Ye.V. Repik and collaborators on establishing relations between the spectra of velocity and temperature (Refs. 37-41) have been described in Appendix II.

### 1.3.3. Spectra

In essence, it is shown in the cited references that a parameter, B, may be constructed as follows, that is nearly constant across a boundary layer.

$$B = \frac{\overline{q^2}}{\theta^2} \left| \frac{\partial T}{\partial \chi_2} / \frac{\partial U}{\partial \chi_2} \right| \quad (3.19)$$

The numerical value of B from experiments is cited as 1.5 in the case. One can compare this equation with Eq. 3.8.

The transfer terms have been modeled in Refs. X and X by writing,

$$\overline{\theta u_j} = a_\theta \left[ \overline{\theta^2} (-\overline{u_i u_j}) \right]^{1/2}$$

It follows than that

$$B = Pr_T a_\theta / a^{1/2} \quad (3.20)$$

The turbulent Prandtl number is defined as

$$Pr_T = \left[ \overline{u_i u_j} / \overline{\theta u_j} \right] \left[ \frac{\partial T}{\partial y} / \frac{\partial U_1}{\partial y} \right] \quad (3.21)$$

and the argument is that  $Pr_T$  is not necessarily constant across the boundary layer.

The authors cited above have also obtained co-spectra for  $u$  and  $\theta$ , but, in fact, conclude that the governing parameter is  $\overline{q^2}$ .

#### I.3.4. Correlations in the Near-Wall Region

It may be recalled that the physical case dealt with by N. Aubry pertains to the structure of flow in the near wall region of a boundary layer. An interesting possibility in the case of heat transfer is that low speed streaks tend to be heated when the boundary plate is heated and high speed streaks may consist of relatively cold fluid arriving from elsewhere. Now, if the low and the high speed streaks are not dynamically interchangeable, heat transfer must change in all cases, and the structure itself should change where there are density changes.

In the context of applying the LEIH to heat transfer problems, it is of interest to have some guidance from experiments on the spectra of  $u$  and  $\theta$ . Several observations in this connection are: (1) There is near-perfect correlation between  $u_i$  and  $\theta$  at the wall. (2) The correlation becomes reduced as one moves out-wards, and (3) at  $y^+ \geq 16$ , there is greater correlation between spectra of the three velocity correlations than between spectra of longitudinal velocity fluctuation and temperature fluctuation. There is close similarity between frequency spectra of velocity and temperature around  $y^+ \approx 2.7$ .

There is also some evidence from cross-spectral data that the correlation between  $u_i$  and  $\theta$  is 'good' at low wave numbers. As  $y^+$  increases, the wave number range over which spectral coherence is constant between  $u_i$  and  $\theta$  increases; spectral coherence is defined by

$$\text{Coh} = (C_0^2 + Q^2) \phi_u \phi_\theta \quad (3.22)$$

$C_0$  = co-spectrum between  $u$  and  $\theta$

$\phi$  = spectral density of fluctuation normalized such that

$$\int_0^\infty \phi(\omega) d\omega = 1$$

### I.3.5. Spectra in the Logarithmic Law Region

We may note from Ref. X that it is possible to conclude that the spectra of  $u$  and  $\theta$  are independent of  $y$  in the log-law region. Further the velocity spectrum and the temperature spectrum are each governed by the  $K^{-1}$  law.

The main conclusion of this section is that spectral similarity between  $\overline{q^2}$  and  $\overline{\theta^2}$  can be invoked provided attention is also paid to the variation of mean velocity and temperature across the boundary layer.

Finally, one can introduce the concept of similarity in spectra and determine mean temperature distribution and hence the skewness factor for temperature fluctuation and  $\gamma_T$  as also the pdf. They can be compared with available experimental data on skewness factor and pdf. In the alternative, one can formulate the temperature problem in the same form as the velocity problem and introduce a skewness factor for temperature and  $\gamma_T$  to obtain a solution. The resulting spectra for velocity and temperature can then be compared with available experimental data. It appears that the latter procedure is likely to be more difficult than the first.

## I.4. PROSPECTS FOR FURTHER RESEARCH

The main conclusions from the current project are the following.

(i) As a prelude to large eddy simulation and full Navier-Stokes equation solvers, the large eddy interaction hypothesis provides a relatively simple basis for establishing interaction between FST and BLT in a fully developed, zero-pressure gradient, low speed TBL. The modelling

involved is unambiguous and is related to two factors, one in the nature of providing an excitation in the dynamical equation for the representative, large eddy and the other in the nature of a damping or dissipation factor.

(ii) The uniqueness of a TBL rests on the unavoidable need for a logarithmic law-governed part of the mean velocity profile. The emergence of such a layer is often a crucial test for the success of a prediction scheme applied to a TBL. When FST is present, it has been found numerically that a number of solutions are feasible with given boundary conditions. The physically valid TBL solution is one of them but require a major feature of boundary layer to be incorporated into the formalism. Two possibilities for such a major feature have been considered: (i) the absence of a pressure gradient to first order in the TBL and (ii) the presence of a logarithmic law-governed layer. Regarding the first, there is still ambiguity in being able to account for the influence of pressure fluctuations in the free stream. On the other hand, regarding the second, only the existence of the region is required and not its extent, which is in fact a part of the solution.

On the other hand, the essential nature of interaction between IST and BLT has remained largely unclear. Experimental data are still to be generated even in the case of interaction between isotropic FST (intensity and scale) and fully developed TBL in respect of the following.

- (i) Appearance of coherent structures and associated phenomena in streamwise and spanwise directions;
- (ii) mean velocity and stress distribution profiles;
- (iii) signature of pressure fluctuations at the walls; and
- (iv) modifications in intermittency, both internal and at outer edge of boundary layer.

Such data are urgently needed for elucidation of the effects of interaction. We have emphasized in the past the significance and

importance of conducting such investigations with free stream turbulence that includes "peaks" in the standard, uniform gauze-generated turbulence.

In the Part II of this Report, the question of establishing free stream turbulence with clearly definable features (in spectrum, space and time) has been addressed. It is found that the setting up of a definable flowfield is not simple and generally involves some ambiguity.

In regard to modelling the interaction, it is useful to proceed as usual to distinguish between the pointwise statistical and the large scale physical structural approaches. However, a common link between the two is the problem of determining what part of FST is in the nature of "inactive" motions, giving rise neither to stresses nor pressure fluctuations. The problem is equivalent to that of determining what part of FST couples with BLT. In respect of this, one may examine the case of a laminar boundary layer in the presence of FST. Experimental evidence exists in sufficiently low Reynolds number flow wherein the mean velocity profile, wall shear stress and heat transfer are affected by FST without the appearance of transition to turbulent flow. This then represents the case of a LBL that (a) creates a balance between production and dissipation of turbulence, both of small magnitude and (b) reduces momentum deficit in itself through acceleration due to turbulent kinetic energy of the free stream. Detailed experimental data and analysis should clarify the features of interaction in this case, which should also throw light on the interaction between FST and TBL.

A question of general import pertains to the rational description of turbulence in terms of vorticity fluctuations. The large eddy interaction scheme has been developed both for velocity fluctuations and correlations, but not for vorticity fluctuations. However, the modelling of interactions between various modes continues to be ad hoc in nature. In the current analysis, for example, the skewness factor and the turbulent viscosity factor cannot be realized directly from experimental data.

A valuable direction for future work on incorporating the physics of turbulence structure as directly as possible into modelling appears to be to

revisit the ideas of the single roller eddy due to Townsend and the intermittency of turbulent processes and entrainment due to Kovaszny. These ideas provide a framework for examining, especially, interactive fluid and thermal fields. The physics itself probably will remain conceptual in various respects.

## REFERENCES

1. Bradshaw, P.: Effects of Free-Stream Turbulence on Turbulent Shear Layers, ARC Report No. 35648, 1974.
2. Hunt, J.C.R., and Graham, J.M.R.: Free-Stream Turbulence near Plane Boundaries, J. Fluid Mech., Vol. 84, 1978.
3. Ahmed, Q.A., Luxton, R.E., and Antonia, R.A.: The Effect of External Turbulent Uniform Shear Flow on a Turbulent Boundary Layer, in Turbulence in Internal Flows, ed. S.N.B. Murthy, Hemisphere, Washington, D.C., 1976.
4. Repik, Ye. U., and Sosenko, Yu. P.: Quantitative Analysis of Intermittency in the Near-Wall Region of a Turbulent Boundary Layer, Fluid Mechanics - Soviet Research, Vol. 16, 1987.
5. Blair, M.F., and Werle, M.J.: The Influence of Free Stream Turbulence on the Zero Pressure Gradient Fully Turbulent Boundary Layer, UTRC Report No. R 80-914388-12, Sept. 1980.
6. Gartshore, I.S., Dubin, P.A., and Hunt, J.C.R.: The Production of Turbulent Stress in a Shear Flow by Irrotational Fluctuations, J. Fluid Mech., Vol. 137, 1983.
7. Wittig, S., et al : Effects of Wakes on the Heat Transfer in Gas Turbine Cascades, AGARD-CP-390, Paper No. 6, 1985.
8. Simonich, J.C., and Bradshaw, P." Effect of Free Stream Turbulence on Heat Transfer through a Turbulent Boundary Layer, J. Heat Transfer, Vol. 100, No. 1978.

9. Becker, B., and River, R. : Computations of the Flowfield and Heat Transfer in a Rectangular Passage with a Turbulator, 34th Gas Turbine Conference, Toronto, ASME Paper No. 89-GT-189, June 1989.
10. Macmullin, R., Elrod, W., and Rivir, R.: Free Stream Turbulence from a Circular Wall Jet on a Flat Plate Heat Transfer and Boundary Layer Flow, The J. Turbomachinery, Vol. 111, Jan. 1989.
11. Miyazaki, H., and Sparrow, E.M. : Analysis of Effects of Free Stream Turbulence on Heat Transfer and Skin Friction, Trans. ASME J. Heat Transfer, Vol. 99, Nov. 1977.
12. Jumper, G.W., Elrod, W.C., and Rivir, R. : Film Cooling Effectiveness in High Turbulence Flow," in Heat Transfer in Gas Turbine Engines, ASME Heat Transfer Division, Vol. 120, 1988.
13. Pouguet, A. and Frisch, U., and Chollet, J.P.: Turbulence with a Spectral Gap, Phys. Fluids, Vol. 28, 1983.
14. Lumley, J.: The Structure of Inhomogeneous Turbulent Flows, Atmospheric Turbulence and Radio Wave Propagation, ed. A.M. Yaglom and V.L. Tatarsky, NAUKA, Moscow, 1967.
15. Lumley, J.: Coherent Structures in Turbulence, in Transition and Turbulence, ed. R.E. Meyer, Academic Press, New York, 1981.
16. Payne, F.R., and Lumley, J.L.: Large Eddy Structure of the Turbulent Wake behind a Circular Cylinder, Phys. Fluids (supplement) Vol. 10, 1967.
17. Leib, S.J., Glauser, M.N., and George, W.K. : An Application of Lumley's Orthogonal Decomposition to the Axisymmetric Turbulent Jet Mixing Layer, Proc. 9th Rolla Symposium, 1986.

18. Glauser, M.N., Leib, S.J., and George, W.K.: Coherent Structures in Axisymmetric Jet Mixing Layer, Proc. 5th Symp. Turb. Shear Flow, Cornell, 1985.
19. Moin, P.: Probing Turbulence via Large Eddy Simulation, AIAA-84-0174, January, 1984.
20. Hong, S.K.: Large Eddy Interactions in Curved Wall Boundary Layers, Ph.D. Thesis, Purdue University, Aug. 1983.
21. Hong, S.K., and Murthy, S.N.B.: Pressure-Strain Correlations in Curved Wall Boundary Layers, AIAA J. Vol. 24, June 1986.
22. Hong, S.K., and Murthy, S.N.B.: Effective Velocity of Transport in Curved Wall Boundary Layers, AIAA J. Vol. 24, March 1986.
23. Hong, S.K.: Large Eddy Interactions in a Turbulent Channel Flow, NASA Tech. Memo. 86757, Sept. 1985.
24. Hong, S.K. and Payne, F.R.: Large Eddy Interaction Models: Potential Turbulent Design Tools, TRL/AE Report No. 88-01, Dept. of Aerospace Engg., Univ. of Texas, Arlington, August, 1988.
25. Hancock, P.E.: The Effect of Free Stream Turbulence on Turbulent Boundary Layers, Ph.D. Thesis, University of London, July 1980.
26. Hancock, P.E., and Bradshaw, P. : The Structure of Turbulent Boundary Layer beneath a Turbulent Free Stream, 6th Symposium on Turbulent Shear Flows, Toulouse, Sept. 1987.
27. Tennekes, T.: AIAA J., Vol. 6, 1968.
28. Yagnik, K.S.: J. Fluid Mech., Vol. 42, 1970.
29. Mellor, G.L.: The Large Reynolds Number, Asymptotic Theory of Turbulent Boundary Layers, Int. J. Engng. Sci., Vol. 10, 1972.

30. Murthy, S.N.B.: AFOSR Semi-Annual Technical Report No. AFW/MB/88-2 Sept. 1988, and AFOSR Semi-Annual Report No. AFW/MB/89-1, Sept. 1989.
31. Robinson, S.K.: A Perspective on Coherent Structures and Conceptual Models for Turbulent Boundary Layer Physics, AIAA 90-1638, June 1990.
32. Donaldson, C. du. P., Sullivan, R.D., and Rosenbaum, H. : AIAA J., Vol. 10, 1972.
33. Gibson, M.M., and Launder, B.E.: Trans. ASME, Vol. 98, 1976.
34. Bradshaw, P., Ferris, D.H., and Atwell, N.P.: Calculation of Boundary Layer Development using the Turbulent Energy Equation, J. Fluid Mech., Vol. 28, 1967. And NPL Aero Report No. 1271, 1968.
35. Townsend, A.A.: The Structure of Turbulent Shear Flow, Second Edition, Cambridge University Press, 1976.
36. Corrsin, S.: J. App. Phys., Vol. 23, 1952.
37. Monin, A.S., and Yaglom, A.M.: Statistical Fluid Mechanics, MIT Press, 1971.
38. Kader, B.A., and Yaglom, A.M.: Spectra of Anisotropic Turbulent Velocity and Temperature Fluctuations in Turbulent-Wall Flows, Fluid Mechanics - Soviet Research, Vol. 16, 1987.
39. Fulachier, L., and Dumas, R.: Spectral Analogy between Temperature and Velocity Fluctuations in a Turbulent Boundary Layer, J. Fluid Mech., Vol. 76, 1976.

40. Fulachier, L., and Antonia, R.: Spectral Analogy between Temperature and Velocity Fluctuations in several Turbulent Flows, Int. J. Heat Mass Transfer, Vol. 27, 1984.
41. Antonia, R.A., Krishnamoorthy, L.V. and Fulachier, L.: Correlation between the Longitudinal Velocity Fluctuation and Temperature Fluctuation in the Near-Wall Region of a Turbulent Boundary Layer, Int. J. Heat Mass Transfer, Vol. 31, 1988.



**AIAA 90-1503**

**Turbulent Boundary Layer with  
Free Stream Turbulence**

S.N.B. Murthy            and    S.K. Hong  
Purdue University            PEDA Corporation  
W. Lafayette, IN              Palo Alto, CA

**AIAA 21st Fluid Dynamics, Plasma Dynamics  
and Lasers Conference**

June 18-20, 1990 / Seattle, WA

## INTRODUCTION

The presence of free stream turbulence in practical, wall-bounded flows is a common occurrence. Whether the wall boundary layer is laminar or in some state of development as a turbulent layer, some form of coupling between free stream turbulence (FST) and boundary layer rotational field can be surmised in all cases except when the scale and intensity of FST are very small. Although specific numerical limits can only apply in particular classes of flows, one can identify low, moderate and high FST as shown schematically in figure 1. In addition to scale and intensity, FST may also display inhomogeneity, for example a spectral gap or peakiness at various wave numbers, as shown in figure 2. The overall problem of establishing the effects of FST must, in general, include both the states of free stream and FST and that of the boundary layer (laminar, transition and turbulence) and also, of the pressure gradient, wall geometry and surface roughness. In the current investigation, we confine attention to interactions between an incompressible, zero pressure gradient turbulent boundary layer and nearly isotropic, moderate FST. Since an adiabatic wall is assumed with no heat transfer, the current case represents a simple interaction between BLT and FST. Experimental data in such a flow configuration are available in Refs. 1 & 2.

The problem of predicting the development of a turbulent boundary layer continues to be challenging (Refs. 3-4). When FST is present, the complexity involved is the interaction of a random vortex fields with one that has a characteristic structure in a random field. The extent to which organized structure becomes changed in a TBL on account of FST has not been established experimentally to date. A beginning investigation has been reported in Ref. 1 wherein, through the use of a hot/cold discrimination technique, a burst frequency has been defined and determined as the average number of hot intervals per unit time (when the boundary wall was mildly heated relative to the free stream) and the burst frequency has been found to vary directly with FST intensity and inversely with its scale. A method of utilizing such data in a predictive scheme can be visualized, but more about this later. Meanwhile, it is clear that a method akin to large eddy simulation (LES) is probably required in order to account fully for the random vorticity field interactions.

In this connection, the rational representation of turbulence suggested by Lumley (Refs. 5-6) as a means of examining eddy-mean shear and eddy-eddy interactions, has been chosen here for application. The authors have some experience with its application to boundary layer flows (Refs. 7-10). The rational representation has been utilized to establish characteristic structures in a channel flow (Ref. 11), and also to obtain the structure of wall layer in a boundary layer (Ref. 12). The Lumley representation has been utilized here entirely at the statistical level to determine the classical structure of TBL with FST.

### LARGE EDDY INTERACTION HYPOTHESIS

The basis of statistical turbulence representation is the Loeve orthogonal decomposition theorem by means of which the velocity fluctuation is expressed in the form of generalized Fourier series:

$$u_i = \sum_{n=1}^{\infty} \alpha_n \phi_i^{(n)}(\underline{x}, t) \quad (1)$$

where  $n$  represents the modes,  $1, 2, 3, \dots$ ,  $\alpha_1, \alpha_2, \alpha_3, \dots$  are random coefficients with units of velocity, uncorrelated with one another.  $\phi_i^{(n)}$  are structure functions, which are furthermore assumed to be orthonormal. The orthogonality condition implies that none of the  $\phi_i^{(n)}$  is identically zero. It follows that

$$\overline{\alpha_n} = 0 \quad (2.1)$$

$$\overline{\alpha_m \alpha_n} = \lambda^{(n)} \delta_{mn} \quad (2.2)$$

$$\int \phi_i^{(p)} \phi_i^{(q)} d\underline{x} dt = \delta_{pq} \quad (2.3)$$

$$\alpha_n = \int u(\underline{x}, t) \phi_i^{(n)}(\underline{x}, t) d\underline{x} dt \quad (2.4)$$

It is assumed that  $\alpha_1, \alpha_2, \alpha_3, \dots$  are ordered such that

$$\lambda^{(1)} > \lambda^{(2)} > \lambda^{(3)} > \dots > 0.$$

Based on the randomness of  $\alpha_n$  and the orthogonality of  $\phi_i^{(n)}$ , one can write for the two-point correlation,

$$R_{ij}(\underline{x}, \underline{x}'; t, t') = \sum_{n=1}^{\infty} \lambda^{(n)} \phi_i^{(n)} \phi_j^{(n)} \quad (3)$$

and

$$\int R_{ij} \phi_i^{(n)}(\underline{x}', t') d\underline{x}' dt' = \lambda^{(n)} \phi_i^{(n)}(\underline{x}, t) \quad (4)$$

where  $\phi_i^{(n)}$  are eigenfunctions with  $\lambda^{(n)}$  as the eigenvalues. For the turbulent kinetic energy, one can then write

$$\int \frac{1}{2} \overline{u^2} \, d\mathbf{x} \, dt = \frac{1}{2} \sum_{n=1}^{\infty} \lambda^{(n)} \quad (5)$$

It follows that  $\lambda^{(n)}$  represents the kinetic energy content of the entire flow associated with  $\phi_i^{(n)}$  or the  $n$ th mode.

The uniqueness of the decomposition is established through calculus of variations, which yields that each mode must account for the maximum of the energy available. One thus has a rational, unique representation of the velocity fluctuation in terms of a series of characteristic eddies. In a given shear flow, the eddies must interact with one another and with the mean shear during flow development. The immediate problem is partitioning of the energy among the different modes. This can be done either by recourse to experimental data or by truncating the nonlinear interactions. On the other hand, the large eddy interaction hypothesis (LEIH) involves consideration of only the first mode over the entire spectrum and its interactions with the mean shear and all eddies. This is obviously a strong limitation of the predictive scheme presented here.

Based on Navier-Stokes equations, one can set up a dynamical equation for the first mode as follows.

$$\begin{aligned} \frac{\partial \tilde{\phi}_i^{(1)}}{\partial t} + U_j \frac{\partial \tilde{\phi}_i^{(1)}}{\partial x_j} + \frac{\partial U_i}{\partial x_j} \tilde{\phi}_j^{(1)} \\ + \frac{\partial}{\partial x_j} \left\{ \sum_{p=1}^{\infty} \sum_{q=1}^{\infty} \frac{\alpha_1 \alpha_p \alpha_q}{(\lambda^{(1)} \lambda^{(p)} \lambda^{(q)})^{1/2}} \tilde{\phi}_i^{(p)} \tilde{\phi}_j^{(q)} \right\} \\ = \frac{\partial \tilde{\pi}^{(1)}}{\partial x_i} + \nu \frac{\partial^2 \tilde{\phi}_i^{(1)}}{\partial x_j^2} \end{aligned} \quad (6)$$

where

$$\tilde{\phi}_i^{(1)} = \sqrt{\lambda^{(1)}} \phi_i^{(1)} \quad (7.1)$$

$$\tilde{\pi}^{(1)} = -\frac{1}{\rho} \frac{\overline{\alpha_i p}}{\sqrt{\lambda^{(1)}}} \quad (7.2)$$

and, for incompressible flow,

$$\frac{\partial^2 \tilde{\pi}^{(1)}}{\partial x_j^2} = 2 \frac{\partial U_j}{\partial x_k} \frac{\partial \tilde{\phi}_k^{(1)}}{\partial x_j} + \frac{\partial^2}{\partial x_k \partial x_j} \{ \quad \} \quad (8)$$

In Eqns. (6) and (8),  $\{ \quad \}$  represents the eddy-eddy interactions. It is essential to model the term. Among various possibilities, the one chosen here is as follows.

$$\sum_{p=1}^{\infty} \sum_{q=1}^{\infty} \frac{\overline{\alpha_1 \alpha_p \alpha_q}}{(\lambda^{(1)} \lambda^{(p)} \lambda^{(q)})^{1/2}} \tilde{\phi}_1^{(p)} \tilde{\phi}_j^{(q)}$$

$$= \frac{\overline{\alpha_1^3}}{\lambda^{(1) 3/2}} \tilde{\phi}_i^{(1)} \tilde{\phi}_j^{(1)} - \nu_t \left( \frac{\partial \tilde{\phi}_i^{(1)}}{\partial x_j} + \frac{\partial \tilde{\phi}_j^{(1)}}{\partial x_i} \right) \quad (9)$$

Here the first term on the right hand side involves a term with a coefficient in the nature of a skewness factor and the second, one resembling eddy viscosity, a type of damping factor. It may be stated at the outset that the second term with  $\nu_t$  is found to be essential in numerical predictions. The skewness factor is associated with the inhomogeneity of the velocity field and the transfer of energy from regions of high intensity to regions of lower intensity.

### FLOWFIELD MODEL

The flowfield of interest is shown schematically in figure 3 with four interactive regions: viscous layer, matching layer, outer layer and free stream. As stated earlier, it is assumed that the no-slip condition at the wall gives rise to a boundary layer in the traditional sense for the ranges of intensity and scale of the FST present. Accordingly the four regions are described in terms of asymptotic expansions utilizing relevant small parameters. There arise two problems.

First, the appearance of the length scale of FST,  $L_e$ , in addition to the inviscid length scale of the flow,  $l$ : there is no difficulty in constructing the required expansion parameters utilizing  $L_e$ , free stream velocity,  $U_e$ , boundary layer thickness  $\delta$  and the outer region length scale,  $\Delta$ . However, the describing equations involve no physical influence of the FST length scale. Therefore, we have proceeded as follows: a value of  $\delta_{0.995}$  is chosen and the dissipation length scale,  $L_\epsilon$ , is determined corresponding to the given value of FST intensity; and a boundary condition is introduced at the edge of the boundary layer requiring the dissipation length scales in the boundary layer and the free stream to be equal at the interface. In other words, that solution is found which yields a dissipation length scale within the boundary layer equal to that in the free stream. The matched asymptotic expansion-solution procedure is otherwise based on an extension of the method of Refs. 13-14, including the presence of FST. The other problem is concerned with the matching layer. In Refs. 1-2 and 15-16 there is considerable evidence for the existence and persistence of the log law character of the region and also for the transverse growth of the region with FST intensity. In Ref. 4 for the case of an ordinary TBL, one without FST, an attempt

was successful in predicting the existence of a constant stress layer corresponding to the log law region. A coordinate transformation and some related assumptions are difficult to understand. In Ref. 17 the log law character of mean flow variation was prescribed in dealing with an ordinary TBL. When FST is present, as stated above, there is a need to match BLT with FST quantities. In order to assure a turbulent boundary layer type solution, it is then found to be necessary to invoke the boundary layer character in some way. In the current formulation it is assumed that the mean flow in the matching layer is governed by the log law. Prescribing this does not, of course, specify the extent of the log law region or that of the defect region.

### TEST FLOW CONFIGURATION

The flow configuration chosen is described in detail in Refs. 1 and 2. A wind tunnel with a speed of about 16.5 m/sec. was utilized to examine a flat plate boundary layer while the FST intensity and length scales were varied by changing the upstream grids. The maximum intensity at any location has been reported to be about 6 per cent, all such locations yielding  $U_e \theta / \nu$  greater than 2,000. The investigation covered various aspects, but the details regarding the few test cases chosen for prediction are summarized in figures 4-6 and Table I. It is of particular interest to observe (a) the simultaneous influence of intensity and length scale of FST, (b) the persistence and enlargement of the log law character of the matching layer in the boundary layer region, and (c) the magnitude of  $L_\epsilon / \delta_{0.995}$  as a function of  $L_e$ , intensity and Reynolds number.

### FLOWFIELD PREDICTION PROCEDURE

The basic numerical method is a fractional method (Refs. 19, 20) applied to equations for the mean flow and also for the large eddy functions  $\phi_i$ . The describing equations for incompressible, time-dependent flow are written in conservative form. The pressure field is determined from the Poisson equation. The crossflow direction  $z$  is transformed into wave number space  $k$ . The convection terms are transformed with second order Adams-Bashforth differencing, and the viscous terms with implicit second order Crank-Nicolson method. Regarding the grid, a staggered grid is employed for discretization: the  $u$  - component variables are placed on the east-west side of the grid cell, the  $v$  - component ones on the south-north side and the  $w$  - component variables and pressure are located at the cell centers. The resulting Poisson equations are solved implicitly with an elliptic procedure without resorting to an approximate factorization technique.

The mean flow equations are decoupled from the large eddy equations during integration in time by allowing the turbulent transport terms in the mean flow equations to lag by the time step  $\Delta t$  when the mean velocities are being solved at  $t = (t_0 + \Delta t)$ . Meanwhile the large eddy field, interacting with the current mean flow field, is implicitly updated for  $t = (t_0 + \Delta t)$ .

Other aspects of the numerical scheme are described in Appendix I. In general, approximately 300 iterations are required in time at each point in the flowfield for the chosen values of  $S$  and  $v_t$ . Then three sets of matching conditions have to be introduced along the transverse direction invoking the log law character of mean flow in the matching layer. Finally, the calculated flowfield has to be iterated with respect to matching boundaries till the boundary conditions are satisfied. The solution so obtained applies to the free stream turbulence case of given intensity and a dissipation length scale as obtained at the outer edge of the boundary layer.

### Preliminary Investigation

In order to test the procedure, the standard equilibrium boundary layer case, the one equivalent to the Falkner-Skan family of laminary boundary layers, (Ref. 18), was computed for  $Re_\theta$  of 2,500. The convergence of the solution as well as the method of choosing the values of  $S$  and  $v_t$  were found satisfactory. It may be noted that since there is no free stream turbulence in this case, it is adequate to demand convergence of the solution.

## PREDICTIONS AND DISCUSSION

A comparison of experimental data and predictions is presented in respect of the following in various test cases: mean flow in figures 7-11, shear stress variations in figures 12-14 and intensity variations in figures 15-18. Some difficulties in predictions that arose in the beginning at the matching stations were corrected subsequently by an adjustment of the computational grid. It is worth mentioning that it was necessary to utilize two different values for the skewness factor in the  $x$  and  $y$  directions in any given case; however, the values were applicable throughout the boundary layer. On the other hand, the values of  $v_T$  were generally immaterial so long as a non-zero value was included.

### Discussion

The investigation pertains to a turbulent boundary in a free stream of moderate turbulent intensity and scale. The interaction region extends over the scale of FST.

The predictive scheme rests on a number of premises. First, in order to assure a turbulent boundary layer in the presence of FST, the matching layer between the viscous sublayer and the outer layer needs to be specified as governed by the Log Law. This is based on the fact that other types of boundary layers are also feasible in a FST environment, and also on the lack of a mechanistic model of interaction between FST and BLT. Second, the outer edge of the boundary layer is treated as a parameter for establishing matching of turbulence dissipation scales. No distinction is made between the locations where the values of turbulence intensities and mean flow are matched, although the presence of the wall must affect the  $y$  - component of intensity. In the

actual computational work, experimental data were utilized extensively in reducing the trial-and-error procedure required in matching free stream and boundary layer flows. Third, the application of LEIH is based on the representation of turbulence by the first mode following orthonormal-orthogonal decomposition. Furthermore, there is no physical significance to the definition of skewness and eddy viscosity factors.

It is gratifying that a choice of skewness and eddy viscosity factors is adequate for reproducing the main turbulence quantities as measured in an experiment. In the predictions, it has (obviously) been possible to obtain spectra; details are provided in Ref. 21. The main observations from the spectra are (i) the contributions from small wave numbers becomes increased when FST is present, more than those from large wave numbers; and (ii) the changes for  $\overline{v^2}$  are smaller than the changes for  $\overline{u^2}$ .

Acknowledgement: The research was supported under AFOSR Contract No. F49620-87-k-0008, Capt. H. Helin and Dr. J. McMichael, contract monitors. The authors would like to express their appreciation to Professor Peter Bradshaw, Dr. R. River and the contract monitors for several valuable discussions. Dr. S.K. Hong was a visiting scientist at the University while performing this work. Dr. T. Bose provided valuable assistance in performing the computational work.

Table I.

VALUES OF  $S_F$  AND  $v_{TF}$  UTILIZED

	$S_{Fi}$	$S_{Fj}$	$v_{TFi}$	$v_{TFj}$
Case 1	0.8	0.82	0.11	0.10
Case 2	0.92	0.92	0.11	0.10
Case 3	0.91	0.93	0.11	0.10
Case 4	0.90	0.93	0.11	0.10
Case 5	0.93	0.91	0.11	0.10

References

1. Hancock, P.E. "The Effect of Free Stream Turbulence on Turbulent Boundary Layers," Ph.D. Thesis, University of London, 1980.
2. Hancock, P.E. and Bradshaw, P. "The Structure of a Turbulent Boundary Layer Beneath a Turbulent Free Stream," 6th Symposium on Turbulent Shear Flows, Toulouse, Sept. 1987.
3. Rogallo, R.S. and Moin, P. "Numerical Simulation of Turbulent Flows," Ann. Rev. Fluid Tech., 16, 1984.
4. Spalart, P.R. "Direct Simulation of a Turbulent Boundary Layer up to  $Re_\theta = 1,440$ ", J. Fluid Mech., Vol. 187, 1988.
5. Lumley, J.L. "The Structure of Inhomogeneous Turbulent Flows," Atmospheric Turbulence and Radio Wave Propagation, ed. A.M. Yaglom, and V.L. Tatarsky, NAUKA, Moscow, 1967.
6. Lumley, J.L. "Coherent Structures in Turbulence," Transition and Turbulence, ed. R.E. Meyer, Academic Press, New York, 1981.
7. Hong, S.K. "Large Eddy Interactions in Curved Wall Boundary Layers," Ph.D. Thesis, Purdue University, Aug. 1983.
8. Hong, S.K. and Murthy, S.N.B. "Pressure-Strain Correlations in Curved Wall Boundary Layers," AIAA J., Vol. 24, No. 6, June 1986.
9. Hong, S.K. and Murthy, S.N.B. "Effective Velocity of Transport in Curved Wall Boundary Layers," AIAA J., Vol. 24, NO. 3, March 1986.
10. Hong, S.K. "Large Eddy Interactions in a Turbulent Channel Flow," NASA Tech. Memo. 86757, Sept. 1985.
11. Moin, P. "Probing Turbulence via Large Eddy Simulation," AIAA-84-0174.

12. Aubry, N. "The Large Scale Structure of the Near-Wall Region of Turbulent Pipe Flow," Ph.D. Thesis, Cornell University, 1987.
13. Yagnik, K.S. "Asymptotic Theory of Turbulence-Shear Flows", J. Fluid Mech., Vol. 42, 1970.
14. Mellor, G.L. "The Large Eddy Reynolds Number, Asymptotic Theory of Turbulent Boundary Layers," Int. J. Engg. Sci., Vol. 10, 1972.
15. Blair, M.F. "Influence of Free Stream Turbulence on Turbulent Boundary Layer Heat Transfer and Mean Flow Development," Parts I and II, ASME J. Heat Transfer, Vol. 105, Feb. 1983.
16. Charnay, G., Compte-Bellot, G., and Mathiew, J. "Development of a Turbulent Boundary Layer on a Flat Plate in an External Turbulent Flow," AGARD CP 93, Paper No. 27, 1971.
17. Walker, J.D.A., Scharnhorst, R.K., and Weigand, G.G. "Wall Layer Models for the Calculation of Velocity and Heat Transfer in Turbulent Boundary Layers," AIAA-86-0213, January 1986.
18. H. Tennekes and Lumley, J.L. "A First Course in Turbulence," The MIT Press, 1972.
19. Peyret, R., and Taylor, T.D. "Computational Methods for Fluid Flow," Springer, New York, 1982.
20. Kim, Y., and Moin, P. "Application of a Fractional Method for Incompressible Navier-Stokes Equations," NASA Tech. Memo. 85898, March, 1984.
21. Murthy, S.N.B., and Bradshaw, P. Final Report No. MB/AFOSR/90-1 on AFOSR Contract No. F49620-87-k-0008, to be published.

## Appendix I

The mean flow equations are written a conservative form as follows:

$$\frac{\partial U_i}{\partial t} + \frac{\partial}{\partial x_j} (U_i U_j - \overline{u_i u_j}) = - \frac{\partial P}{\partial x_i} + \frac{1}{\text{Re}} \frac{\partial^2 U_i}{\partial x_j^2} \quad (\text{A.1})$$

with

$$\overline{u_i u_j} = \phi_i \phi_j \quad (\text{A.2})$$

The large-eddy functions  $\phi_i$  are governed by the dynamical equation in physical  $(x,y,z)$  space as follows.

$$\begin{aligned} \frac{\partial \phi_i}{\partial t} + \frac{\partial}{\partial x_j} (\phi_i U_j) + \frac{\partial}{\partial x_j} (\phi_i U_j) + S \frac{\partial}{\partial x_j} (\phi_i U_j) \\ = - \frac{\partial \pi}{\partial x_i} + (\nu + \nu_t) \frac{\partial^2 \phi_i}{\partial x_j^2} \end{aligned} \quad (\text{A.3})$$

In the following, the solution procedure is illustrated only for the x-component of  $\phi_i$ . The same procedure can be extended to other components of  $\phi_i$ .

The flow is assumed to be homogeneous in the spanwise  $z$  - coordinate direction. One can then introduce Fourier expansions for velocity and pressure as follows.

$$\phi_i(x,y,z,t) = \sum_{k=-\infty}^{\infty} \hat{\phi}_i(x,y,k,t) e^{\hat{i} k z} \quad (\text{A.4})$$

$$\pi(x,y,z,t) = \sum_{k=-\infty}^{\infty} \hat{\pi}(x,y,k,t) e^{\hat{i} k z} \quad (\text{A.5})$$

where  $\hat{i} \equiv \sqrt{-1}$ . Applying these to Eq. (A.3), one obtains a complex equation for  $\hat{\phi}_i(x,y,k,t)$  as shown below.

$$\begin{aligned}
& \frac{\partial \hat{\phi}_1}{\partial t} + 2 \frac{\partial}{\partial x} (U \hat{\phi}_1) + \frac{\partial}{\partial y} (V \hat{\phi}_1) + \frac{\partial}{\partial y} (U \hat{\phi}_2) \\
& + i k U \hat{\phi}_3 + S \cdot F \left\{ \frac{\partial}{\partial x_j} (\phi_1 \phi_j) \right\} \\
& = - \frac{\partial \hat{\pi}}{\partial x} + (v + v_l) \left( \frac{\partial^2}{\partial x^2} + \frac{\partial^2}{\partial y^2} - k^2 \right) \hat{\phi}_1
\end{aligned} \tag{A.6}$$

where the F - term is equivalent to

$$\begin{aligned}
& \sum_{k' = -\infty}^{\infty} \left\{ \frac{\partial}{\partial x} [\hat{\phi}_1(k') \hat{\phi}_1(k - k')] + \frac{\partial}{\partial y} [\hat{\phi}_1(k') \hat{\phi}_2(k - k')] \right. \\
& \left. + i k \hat{\phi}_1(k') \hat{\phi}_3(k - k') \right\}
\end{aligned}$$

Thus information between a large and a small wave number is exchanged through the convolution term. The solution for  $\hat{\phi}_1$  can then be obtained at time  $t = t_0 + \Delta t$  utilizing the values of mean velocities U and V which have been determined corresponding to that instant but, as stated under Numerical Procedure, with the Reynolds stresses for  $t = t_0$ .

The first step in solving Eq. (A.6) is to determine an intermediate function  $\hat{\phi}_1^*$  from the following equation.

$$\begin{aligned}
& \frac{\hat{\phi}_1^* - \hat{\phi}_1^n}{\Delta t} + U \left\{ \frac{\partial \hat{\phi}_1}{\partial x} + V \frac{\partial \hat{\phi}_1}{\partial y} + \frac{\partial U}{\partial x} \hat{\phi}_1 + \frac{\partial U}{\partial x} \hat{\phi}_2 \right\}^n \\
& + \frac{1}{2} \left\{ 3 \cdot S \cdot F (\phi_1 \phi_j)^n - S \cdot F (\phi_1 \phi_j)^{n-1} \right\} \\
& = \frac{1}{2} \frac{1 + v_l}{\text{Re}} \left( \frac{\partial^2}{\partial x^2} + \frac{\partial^2}{\partial y^2} - k^2 \right) (\hat{\phi}_1^* + \hat{\phi}_1^n)
\end{aligned} \tag{A.7}$$

It is subject to the conditions

$$\hat{\phi}_1^* = \hat{\phi}_1^{n+1} + (\Delta t) \left( \frac{\partial \hat{\pi}}{\partial x} \right)^{n+1} \approx \hat{\phi}_1^{n+1} + (\Delta t) \left( \frac{\partial \hat{\pi}}{\partial x} \right)^n \quad (\text{A.8})$$

Equation (A.8) assumes that  $\hat{\pi}^{n+1} \approx \hat{\pi}^n$  at the boundary and is a second-order approximation in time,  $O(\Delta t^2)$  (Ref. 20). Introduction of  $\hat{\phi}_1^*$  in the viscous term in Eq. (A.8) stabilizes the numerical solution for  $\hat{\phi}_1^*$ . Once  $\hat{\phi}_1^*$  is solved from the elliptic equation (A.8), then the pressure spectra  $\hat{\pi}^{n+1}$  is obtained from

$$\frac{\partial^2 \hat{\pi}}{\partial x^2} + \frac{\partial^2 \hat{\pi}}{\partial y^2} - k^2 \hat{\pi} = \frac{1}{\Delta t} \left( \frac{\partial \hat{\phi}_1^*}{\partial x} + \frac{\partial \hat{\phi}_2^*}{\partial y} + \hat{i} k \hat{\phi}_3^* \right) \quad (\text{A.9})$$

subject to boundary conditions, namely

$$\begin{aligned} \frac{\partial \hat{\pi}^{n+1}}{\partial x} &= \frac{1}{\Delta t} \left( \hat{\phi}_1^* - \hat{\phi}_1^{n+1} \right) \\ \frac{\partial \hat{\pi}^{n+1}}{\partial y} &= \frac{1}{\Delta t} \left( \hat{\phi}_2^* - \hat{\phi}_2^{n+1} \right) \\ \hat{i} k \hat{\pi}^{n+1} &= \frac{1}{\Delta t} \left( \hat{\phi}_3^* - \hat{\phi}_3^{n+1} \right) \end{aligned} \quad (\text{A.10})$$

Finally, updated values for  $\hat{\phi}_1^{n+1}$  are computed directly from

$$\frac{\hat{\phi}_1^{n+1} - \hat{\phi}_1^*}{\Delta t} = - \frac{\partial \hat{\pi}^{n+1}}{\partial x}$$

or

$$\hat{\phi}_i^{n+1} = \hat{\phi}_i^* - (\Delta t) \frac{\partial \hat{\pi}^{n+1}}{\partial x}$$

The intensities and Reynolds stress components  $\overline{u_i u_j}$  are then calculated from  $\hat{\phi}_i$ , integrating over a chosen wave number range as follows.

$$\overline{u_i u_j}(x, y, t) = \int_{-\infty}^{\infty} \hat{\phi}_i(x, y, k, t) \hat{\phi}_j^*(x, y, k, t) dk \quad (\text{A.12})$$

where \* on  $\hat{\phi}_j$  denotes the complex conjugate. It is found that a set of discrete wave numbers encompassing the desired range is adequate in practice.

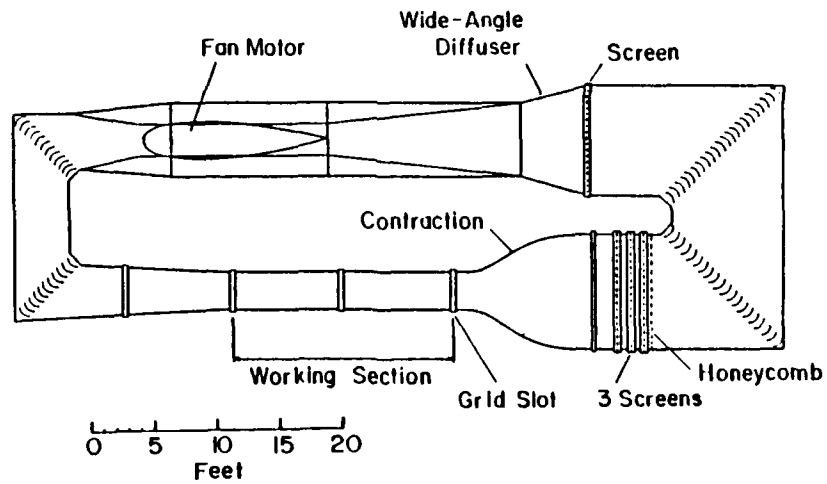
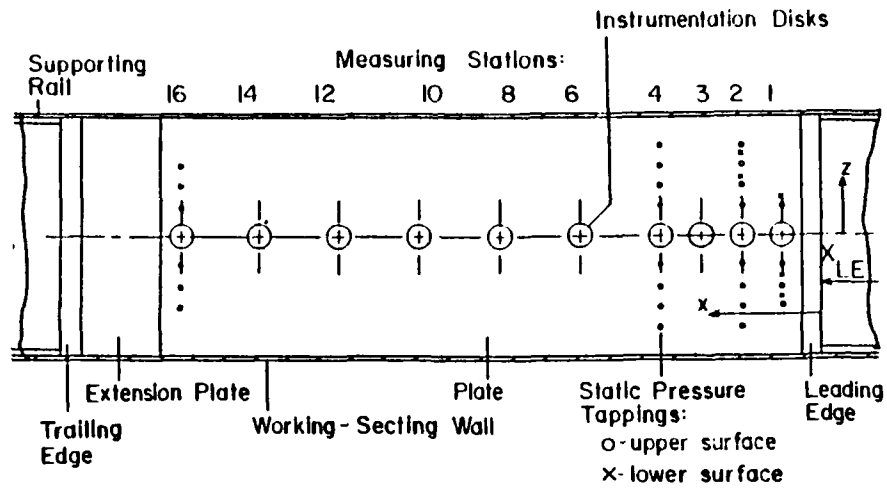
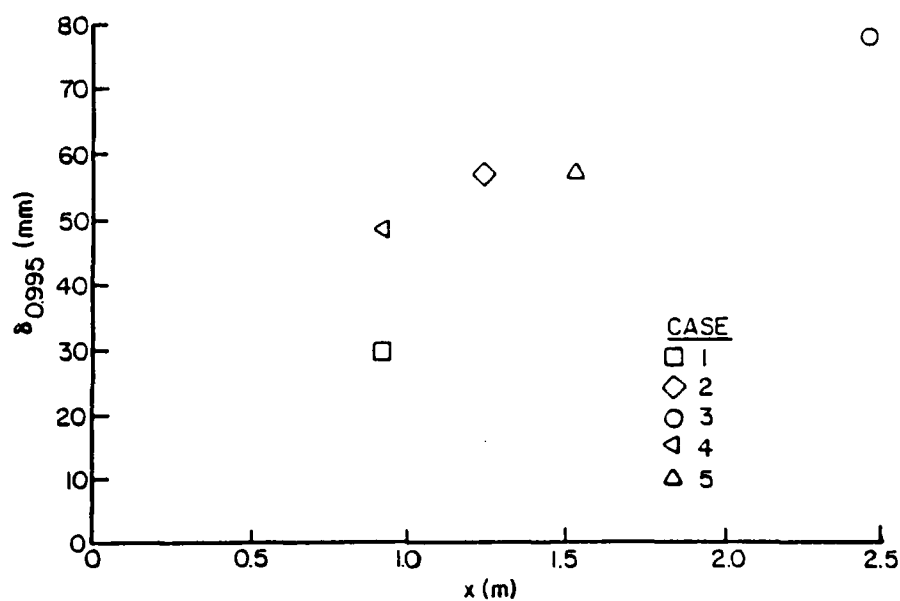
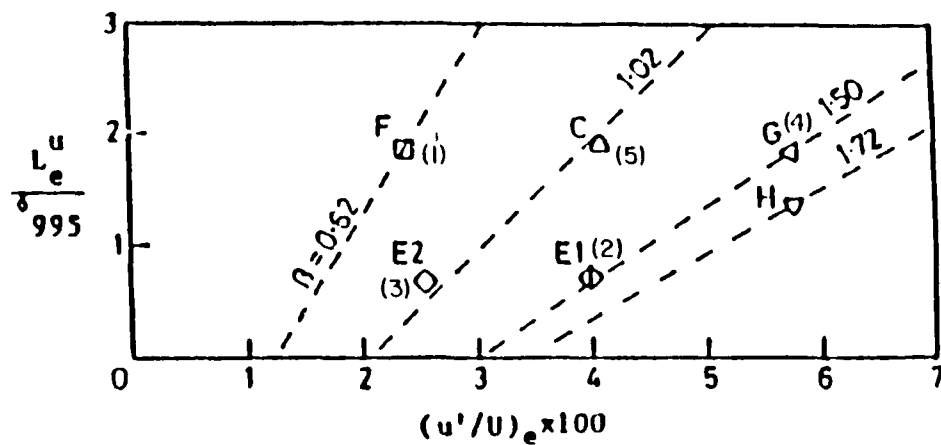


Figure 4. Experimental set-up.



BOUNDARY LAYER THICKNESS  $\delta_{0.995}$  PLOTTED AGAINST  $x$ .

### SELECTED EXPERIMENTAL DATA OF HANCOCK

Case No.	M	$U_e, m$	Station, cm	$\delta_{0.995}, mm.$	$u'/U_e$	$Le^u/\delta_{0.995}$	$Re_\theta$
1	7.6	16	206.2+91.2 <sup>(6)</sup>	29.1	0.0240	1.88	2,980
2	7.6	16	30+121.6 <sup>(8)</sup>	56.9	0.0482	0.71	3,710
3	7.6	16	30+243.2 <sup>(16)</sup>	78.4	0.0255	0.67	5,760
4	15.2	16	152+91.2 <sup>(6)</sup>	48.1	0.0575	1.83	3,100
5	15.2	16	206.2+152.0 <sup>(10)</sup>	56.8	0.0410	1.90	4,320

- Notes:
1. The value of  $U_e$  is nominal with slight variations.
  2. The values of  $\delta_{0.995}$  and  $Re_\theta$  correspond to the no-grid case,  $M = \infty$ .

Figure 5. Test cases 1-5 chosen.

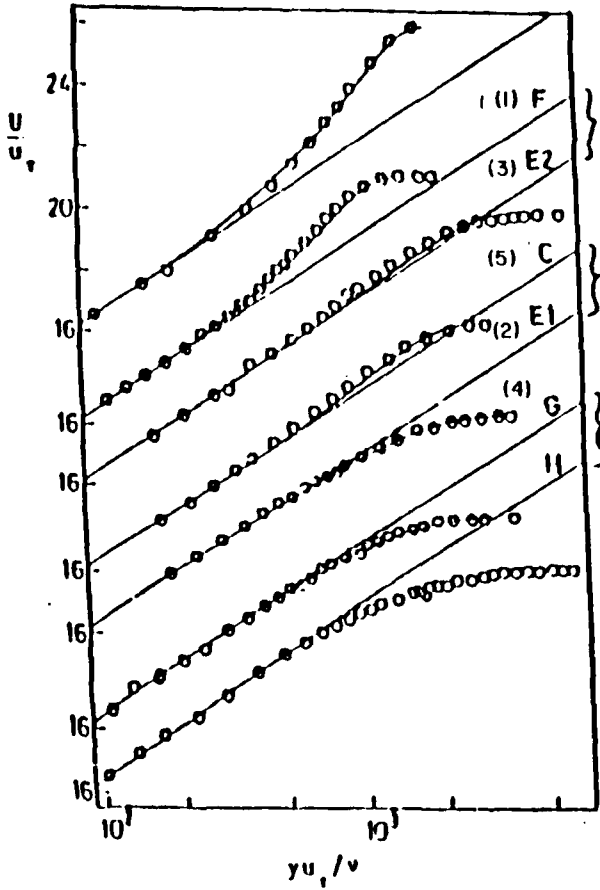


Figure 6. Mean flow profiles in various cases.

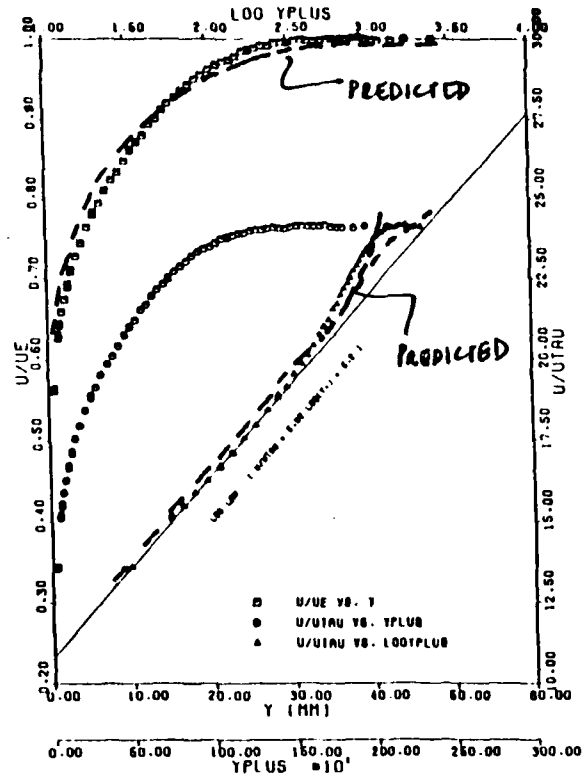


Figure 7. Mean flow prediction: case 1.

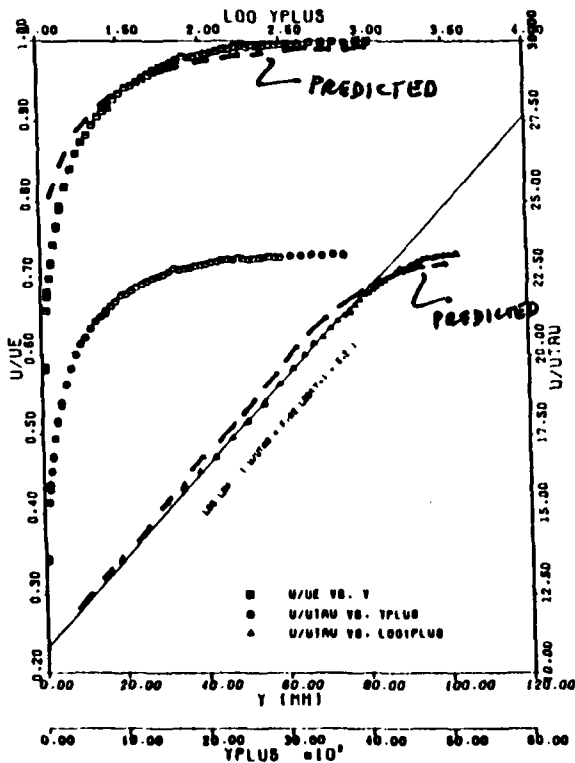


Figure 8. Mean flow prediction: case 2.

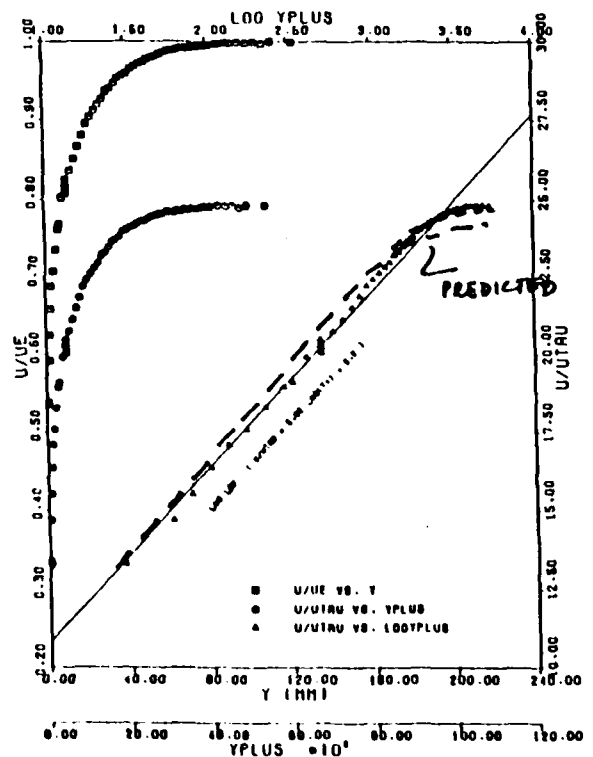


Figure 9. Mean flow prediction: case 3.

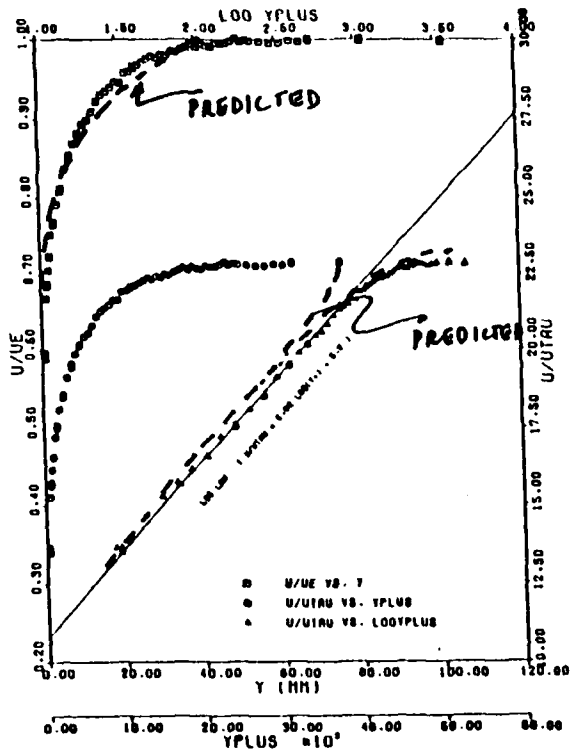


Figure 10. Mean flow prediction: case 4.

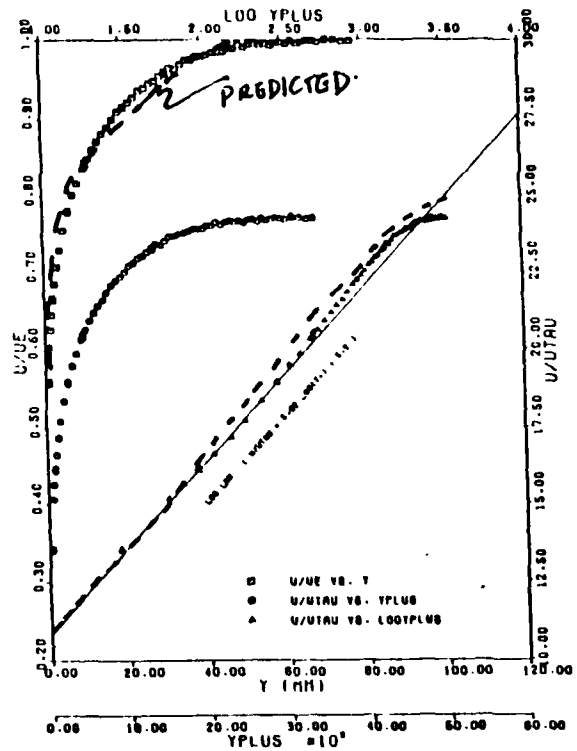


Figure 11. Mean flow prediction: case 5.

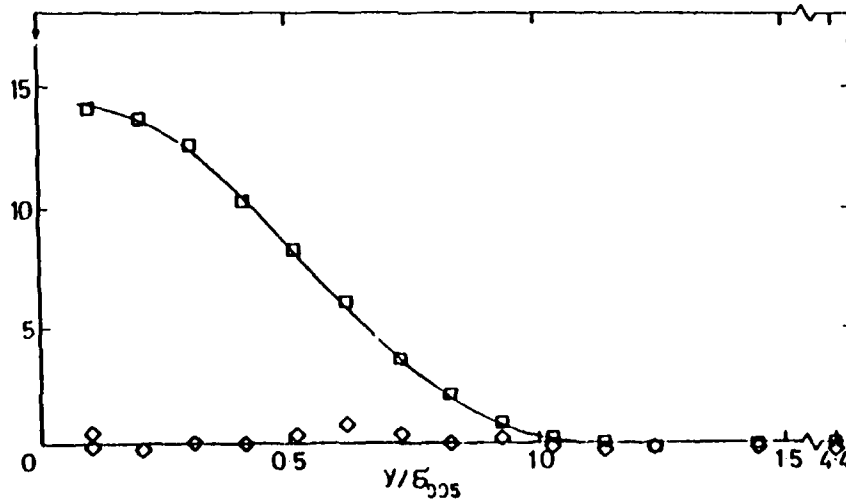


Figure 12. Shear stress prediction: case 1.

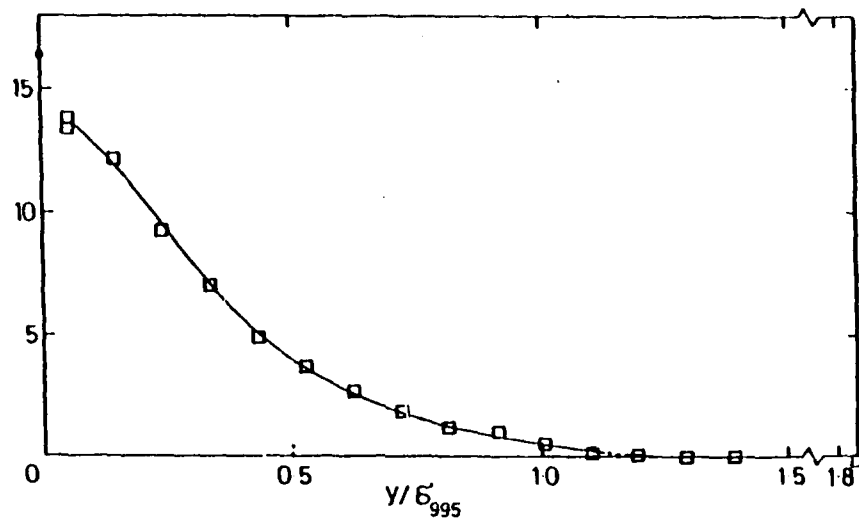


Figure 13. Shear stress prediction: case 2.

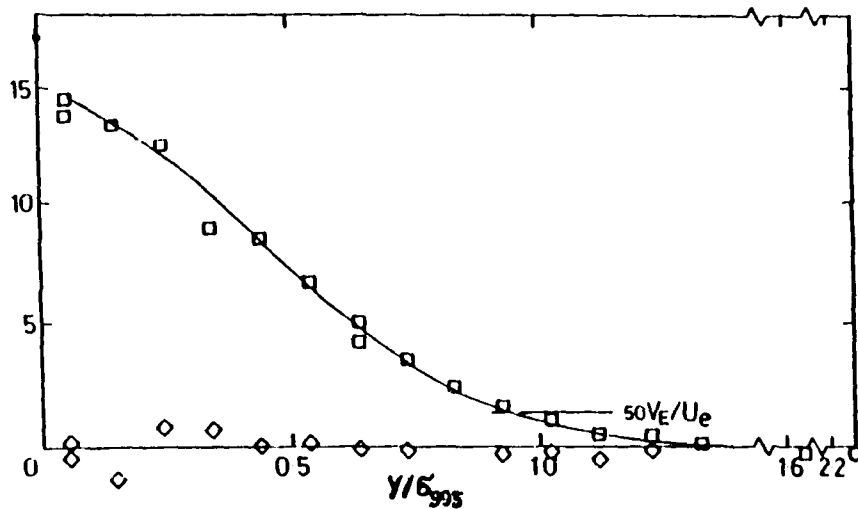


Figure 14. Shear stress prediction: case 5.

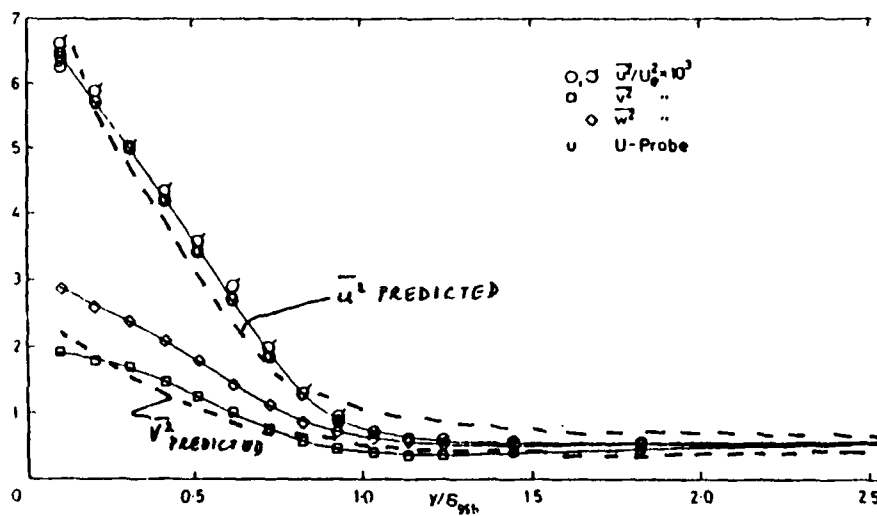


Figure 15. Direct stress prediction: case 1.

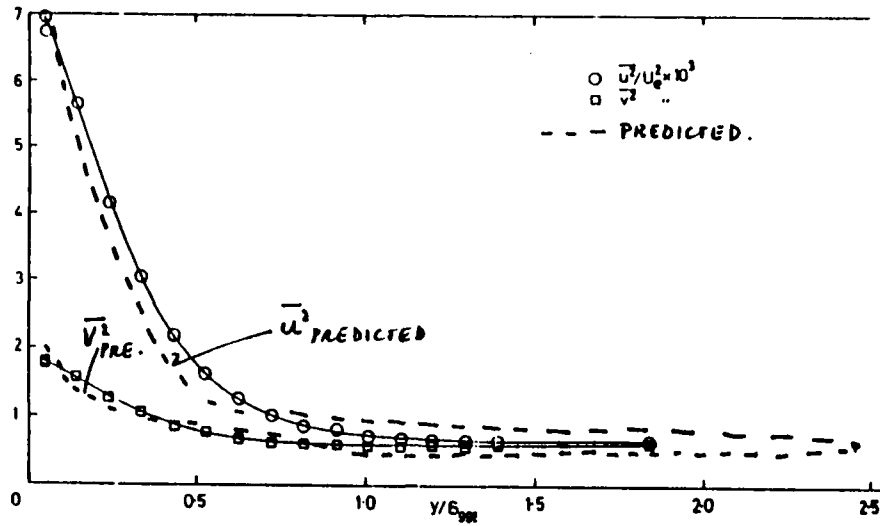


Figure 16. Direct stress prediction: case 3.

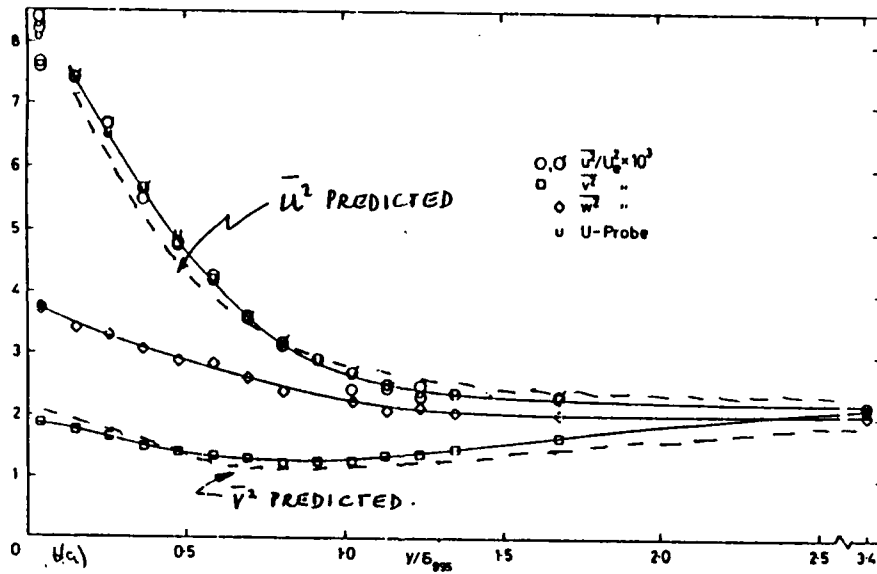


Figure 17. Direct stress prediction: case 4.

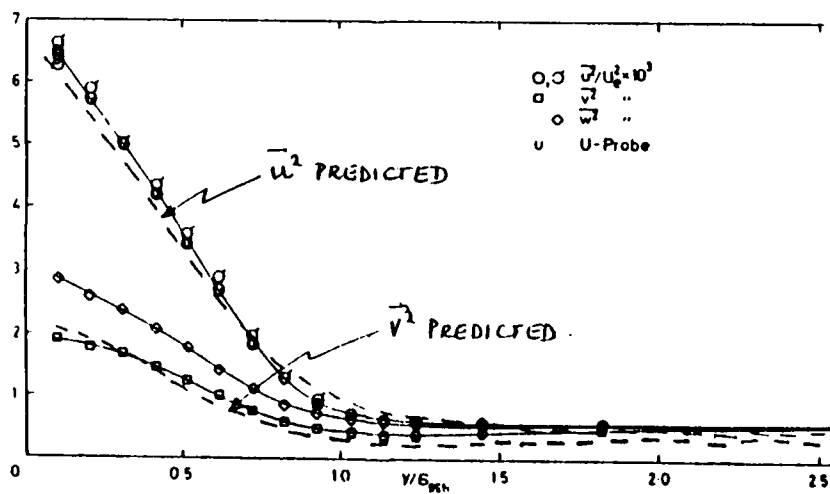


Figure 18. Direct stress prediction: case 5.

TURBULENCE-MEAN DISCONTINUITY IN  
SUPERSONIC FLOW

(Paper accepted for poster-session during the Meeting on The Physics of Compressible Turbulent Mixing, Princeton University, Princeton, NJ, Oct. 24-27, 1988.)

S.N.B. Murthy  
School of Mechanical Engineering  
Purdue University  
West Lafayette, IN 47907

ABSTRACT

An attempt is made to illustrate a relation between large eddy interaction hypothesis and rapid distortion in the context of a shockwave and an expansion interacting with turbulence as depicted in the experimental studies of J. F. Debieve et al., 1982 and J. P. Dussauge, 1981. Spectral analysis is used in computation.

TURBULENCE-MEAN DISCONTINUITY  
IN SUPERSONIC FLOW

S.N.B. Murthy

School of Mechanical Engineering

Purdue University

West Lafayette, IN 47907

ABSTRACT

An attempt is made to illustrate a relation between large eddy interaction hypothesis and rapid distortion approximation in the context of expansion of turbulent supersonic flow, J.F. Debieve et al. 1982 based on J.P. Dussange, 1981. Three cases are compared in relation to pressure-strain correlations, namely (1) sudden expansion, (2) gradual expansion over a curved wall and (3) incompressible flow over a curved wall. The differences between the three cases are illustrated in terms of the portion of the energy spectrum that makes the most contribution to pressure-strain correlations. Similar analysis is underway for velocity-temperature correlations.

Acknowledgement: The research has been supported under AFOSR Contract No. F49620-87-k-0008, Capt. H. Helin as Project Officer.

- BACKGROUND (J.P. DUSSAUGE, 1981).
  - FORMULATION IN MASS-WEIGHTED VARIABLES
  - INTRODUCTION OF VARIABLE THAT ACCOUNTS FOR MEAN DILATION.
  - RAPID DISTORTION
    - DENSITY VARIATIONS FROM MEAN MOTION
    - SOLENOIDAL VELOCITY FLUCTUATIONS
    - SIMILARITY BETWEEN  $U_i$  AND  $\Theta$
    - PRESSURE STRAIN WITH
      - INCOMPRESSIBLE  $p'$  AND
      - $D_{ij}$  INSTEAD OF  $\partial u_i / \partial x_j$
- MAIN RESULTS
  - TURBULENCE INCREASES ACROSS SHOCKWAVE
    - AT HIGH WAVE NUMBER
  - TURBULENCE DECREASES ACROSS EXPANSION
    - WITH UNEXPLAINED BEHAVIOR AT HIGH WAVE NUMBERS
  - INTEGRAL SCALE DEPENDS STRONGLY ON
    - $\rho'$  AND  $\partial \bar{\rho} / \partial x_1$

• PRESSURE-STRAIN,  $\pi_{ij}$  (J.P. DUSSAUGE)

$$-\rho^{2/3} \pi_{ij} = \frac{D}{Dt} (R_o)_{ij} + (R_o)_{ik} D_{jk} + (R_o)_{jk} D_{ik}$$

$R_o$  BEING THE SOLUTION OF

$$\frac{DR}{Dt} + \frac{\partial U}{\partial x} R + R \left( \frac{\partial U}{\partial x} \right)^* = S = 0$$

$$\bullet \Delta p' = -2\bar{\rho} \frac{\partial u_i}{\partial x_j} \frac{\partial U_j}{\partial x_i}$$

$$- \frac{1}{\bar{\rho}} \frac{\partial \rho'}{\partial x_i} \left( \bar{\rho} U_j \frac{\partial U_i}{\partial x_j} \right)$$

$$- \rho' \frac{\partial u_i}{\partial x_j} \frac{\partial U_i}{\partial x_i}$$

$$- \frac{\partial \bar{\rho}}{\partial x_i} \left[ \frac{\partial}{\partial t} u_i + U_j \frac{\partial u_i}{\partial x_j} + u_j \frac{\partial U_i}{\partial x_j} \right]$$

- LARGE EDDY INTERACTION HYPOTHESIS

- DYNAMICAL EQUATIONS FOR

$u_i$  ,  $\Theta$  AND  $p'$ .

- $\nabla p' = -2\bar{\rho} \frac{\partial u_i}{\partial x_j} \cdot \frac{\partial U_i}{\partial x_i}$ .

$$- \frac{\partial \bar{\rho}}{\partial x_i} \left[ \frac{\partial u_i}{\partial t} + U_j \frac{\partial u_i}{\partial x_j} + u_j \frac{\partial U_i}{\partial x_j} \right]$$

under the assumption of linearization and neglect of  $\rho'$ .

- ORTHOGONAL DECOMPOSITION

- FINITE VELOCITY OF TRANSPORT

- SPECTRAL LEVEL ANALOGY BETWEEN  $\bar{u}_i^2$  AND  $\bar{\Theta}^2$ .

- CALCULATION PROCEDURE

- REGION OF INTEREST

- SUPERSONIC FLOW

- BOUNDARY LAYER WAKE
      - OUTER TURBULENT FLOW

- FIND  $\rho'$  FROM  $p'$  and  $\Theta$

- CORRECT  $p'$  for  $\rho'$ .

- FIND  $p' \frac{\partial u_i}{\partial x_j}$

- ESTABLISH SPECTRAL CONTENT

- COMPARE

- RAPID DISTORTION OVER CURVED WALL
        - NORMAL DISTORTION OVER CURVED WALL
        - INCOMPRESSIBLE FLOW OVER CURVED WALL

- TWO SETS OF RESULTS

- LEIH UNDER RAPID DISTORTION APPROXIMATION

- LEIH

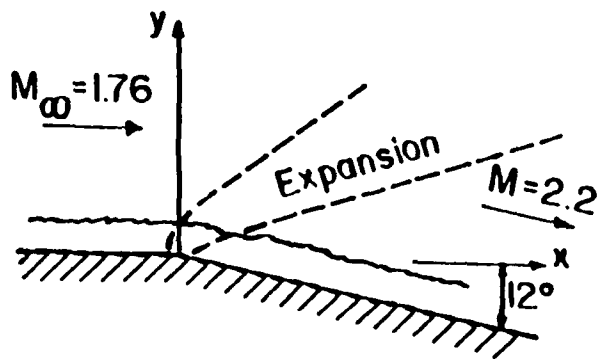
- **MAIN RESULTS**

- **PRESSURE-STRAIN CORRELATIONS SEEM TO PRESENT SOME AMBIGUITIES IN RAPID DISTORTION APPROXIMATION COMPARED TO TURBULENCE INTENSITY.**
- **PRESSURE-STRAIN CORRELATION ESTIMATES SHOW THE EFFECTS OF INACTIVE MOTION WHICH BECOME DECREASED DURING EXPANSION. HOWEVER, DISSIPATION SEEMS TO INCREASE.**
- **RAPID DISTORTION APPROXIMATION YIELDS RESULTS OF DOUBTFUL VALIDITY EXCEPT AT VERY LOW WAVE NUMBERS.**
- **THE LEIH IS SUITABLE FOR EVALUATING COMPRESSIBILITY EFFECTS IN THE PRESENCE OF FREE STREAM TURBULENCE.**
- **THE LEIH MODEL VERIFIES EXPERIMENTALLY OBSERVED DIFFERENCES BETWEEN INNER, OUTER AND FREESTREAM REGIONS.**
- **CORNER EXPANSION YIELDS RESULTS SIMILAR TO RELAXING FLOWS.**
- **CURVATURE DOMINATES OVER EXPANSION EFFECTS.**

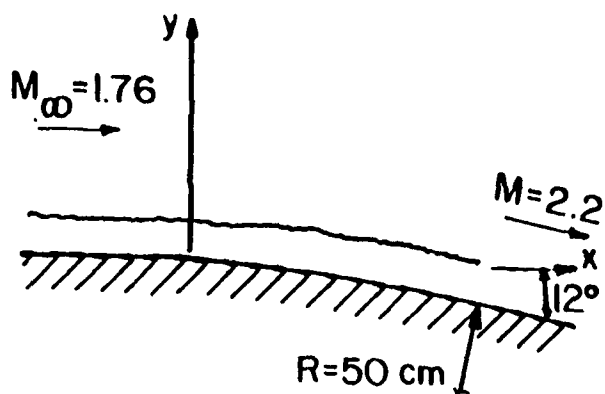
## REFERENCES

- D. BESTION, J.F. DEBIEVE AND J.P. DUSSAUGE: IUTAM SYMPOSIUM, MARSEILLE, FRANCE, 1982.
- M.J. LIDTHILL: GAS DYNAMICS OF COSMIC CLOUDS, p. 121, SYMPOSIUM, CAMBRIDGE, 1949.
- S. CHANDRASEKHAR: PROC. ROY. SOC. 210 A, 18, 1951.
- A.M. SEVILLE: ANN REVS. FLUID MECHANICS, VOL. 19, P. 531, 1987.
- J. LUMLEY: IN TRANSITION AND TURBULENCE, ED. R.E. MEYER, ACADEMIC PRESS, 1981.
- S.K. HONG AND S.N.B. MURTHY: AIAA J., 24 (6) JUNE 1986.

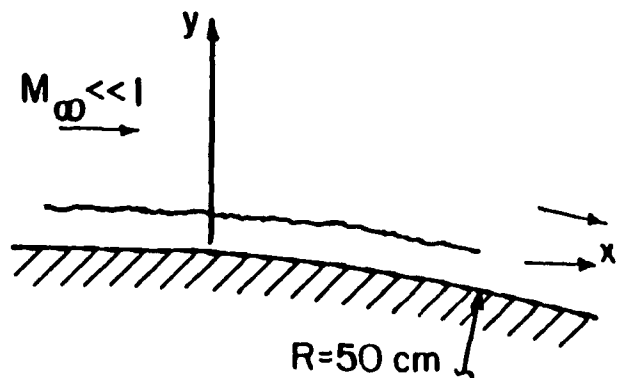
# PROBLEM CONSIDERED



A) RAPID DISTORTION



B) LARGE-EDDY INTERACTION HYPOTHESIS



C) LARGE-EDDY INTERACTION HYPOTHESIS

● COMPARE SPECTRAL CONTENT OF PRESSURE-STRAIN CORRELATIONS.

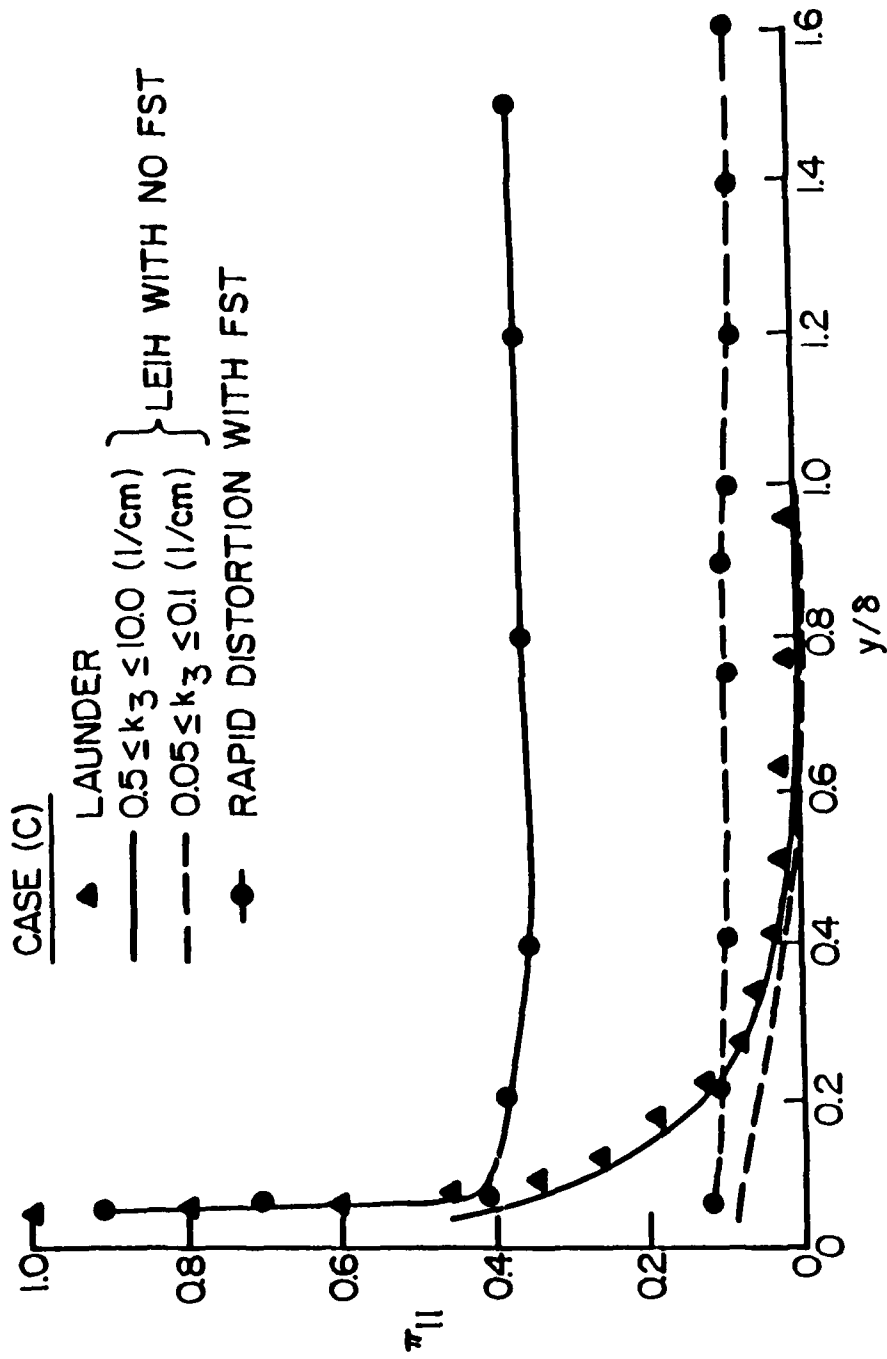


Fig. 1. Normalized distribution of pressure-strain correlation component  $\pi_{||}$  vs.  $y/\delta$  for the strong convex case at  $x=15$  cm.

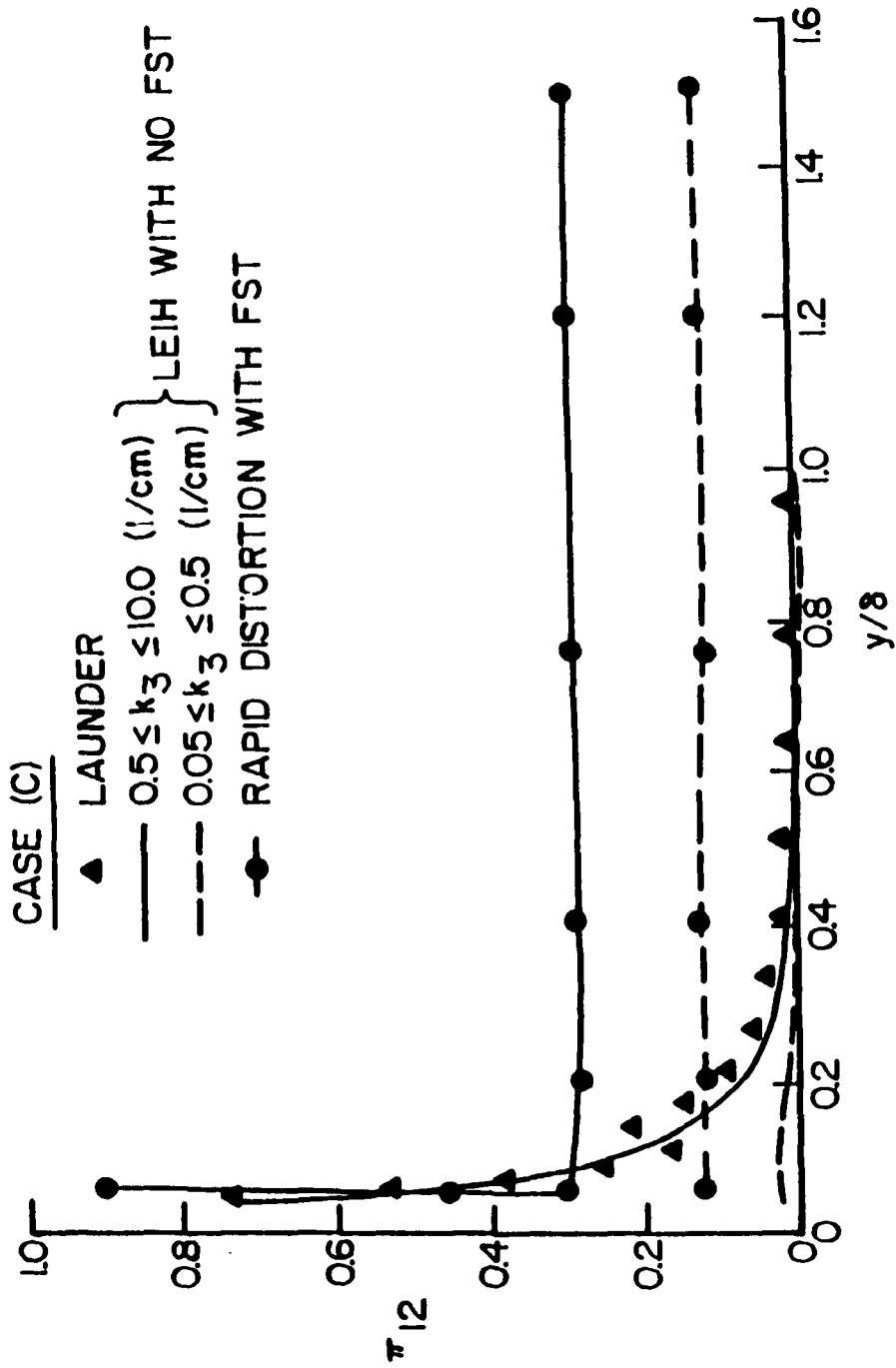


Fig. 2. Normalized distribution of pressure-strain correlation component  $\pi_{12}$  vs.  $y/8$  for the strong convex case at  $x=15$  cm.

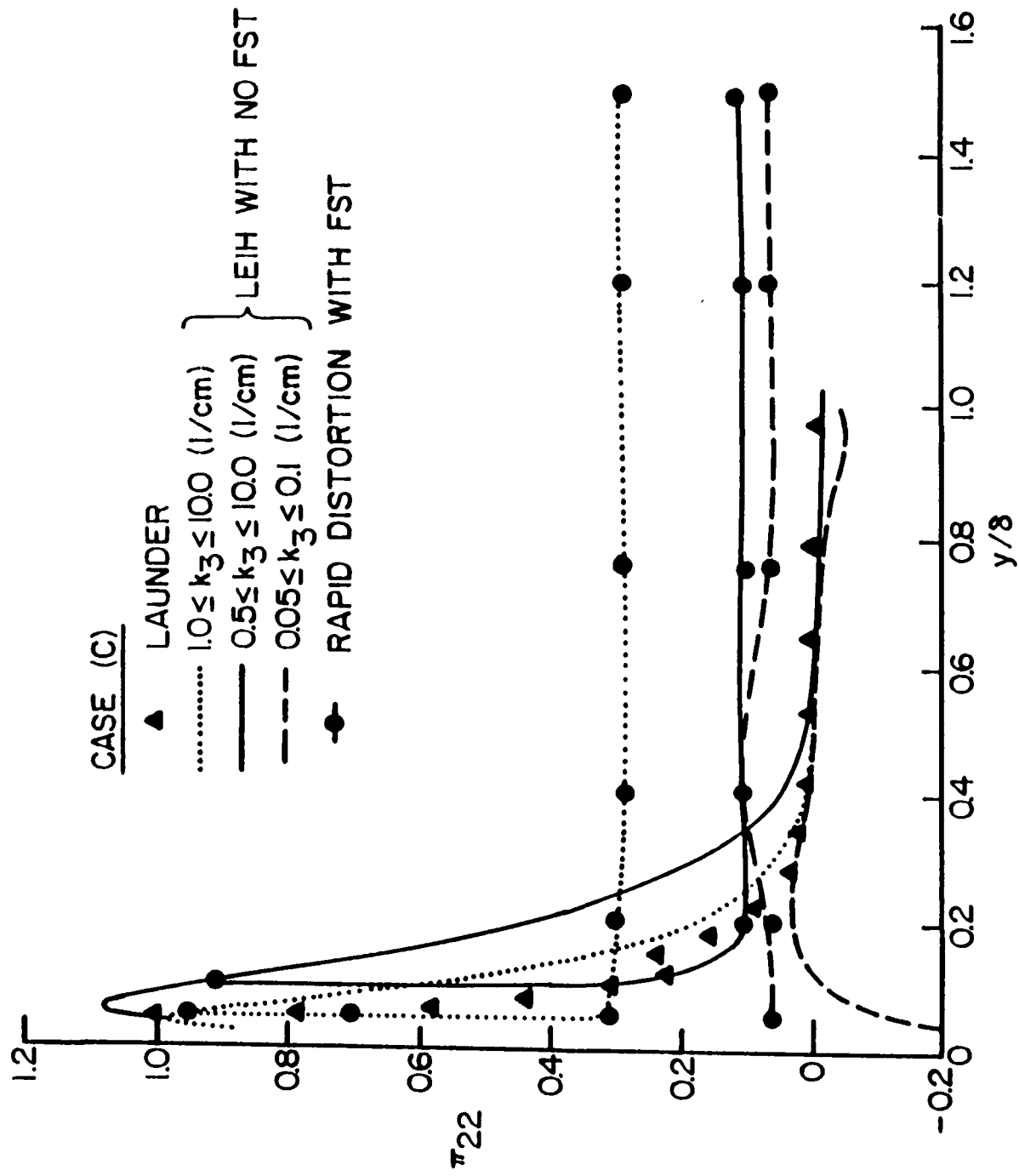


Fig. 3. Normalized distribution of pressure-strain correlation component  $\pi_{22}$  vs.  $y/8$  for the strong convex case at  $x = 15$  cm.

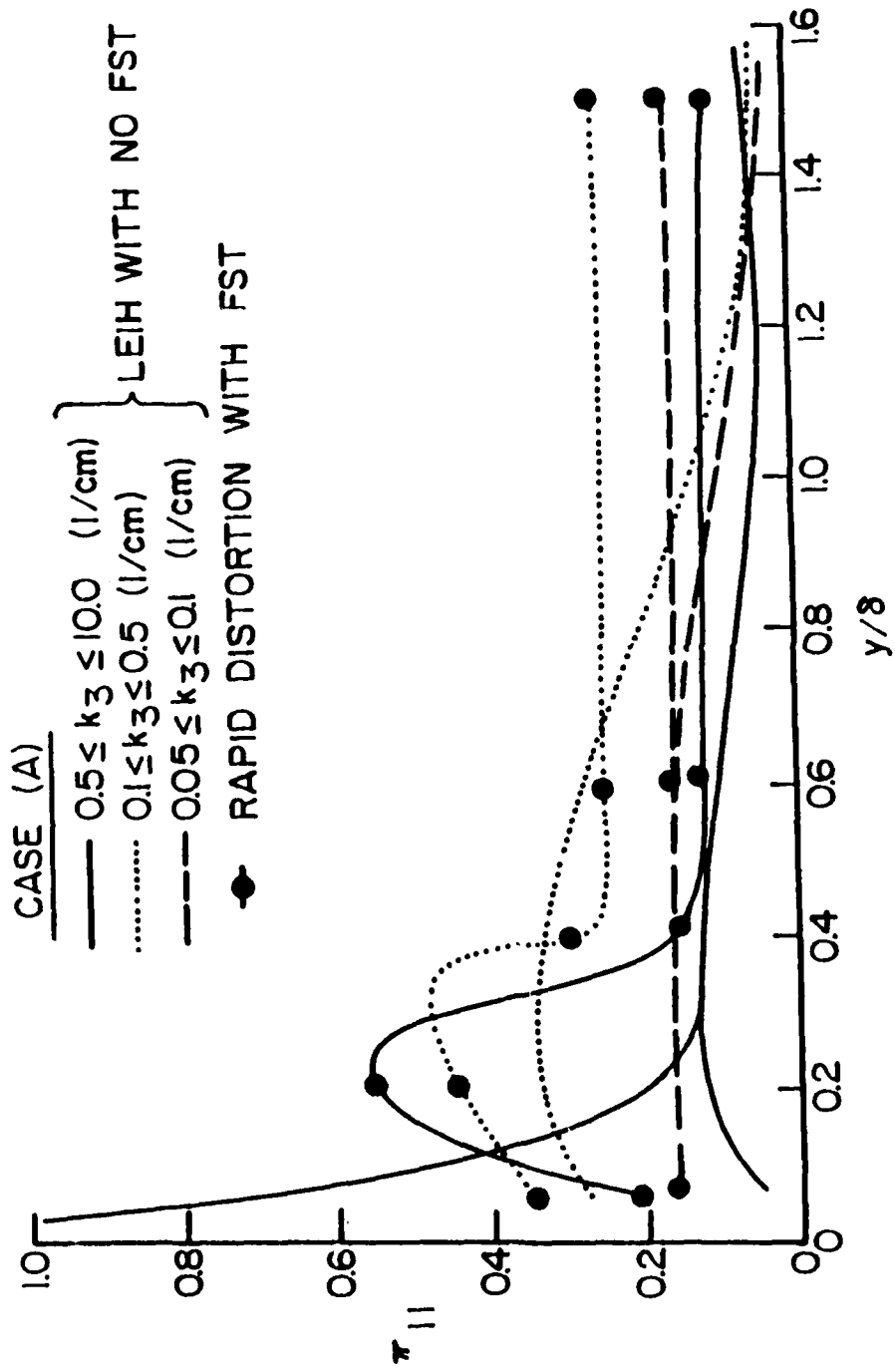


Fig. 4. Normalized distribution of pressure-strain correlation component  $\pi_{||}$  vs.  $y/\delta$  for case (A) at  $x=15$  cm.

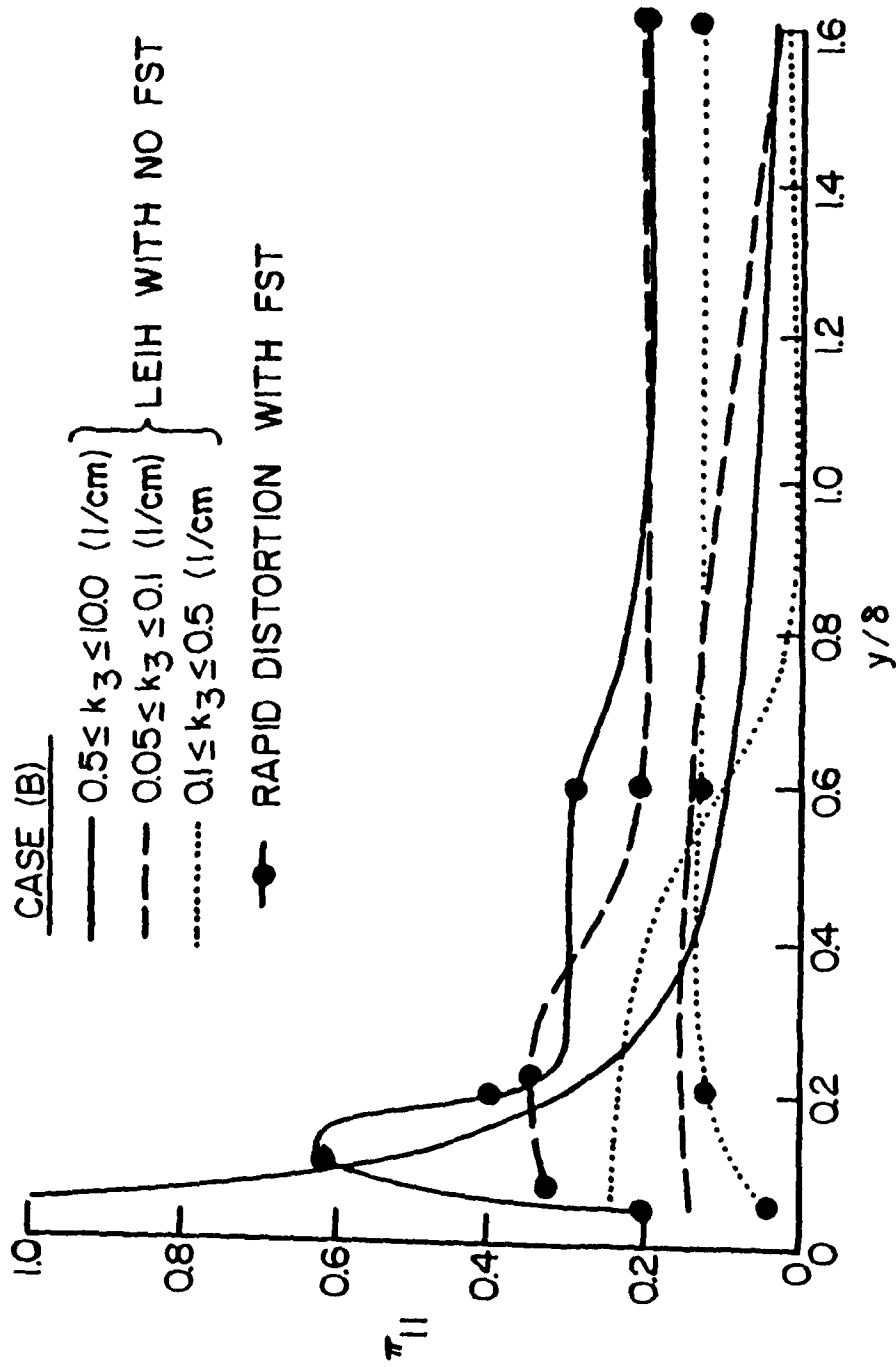


Fig. 5. Normalized distribution of pressure-strain correlation component  $\pi_{||}$  vs.  $y/\delta$  for case (B) at  $x=15$  cm.

PART II

SUMMARY OF IMPERIAL COLLEGE WORK  
ON FREE STREAM TURBULENCE

P. BRADSHAW

TABLE OF CONTENTSPART II

	page
II.1. Introduction	II.1
II.2. Equipment and Techniques	II.2
II.3. Results	II.2
II.3.1. First Stage - Isotropic Free Stream Turbulence	II.2
II.3.2. Second Stage - Wakes of Spanwise Rods	II.2
II.3.3. Third Stage - Wake of a Stationary Inclined Rod	II.3
II.4. Conclusions	II.4

\* Copies of Relevant Publication

Summary of Imperial College work on free-stream turbulence  
(ref. no. 989AQ/AB) under contract with Purdue University.

P. Bradshaw, Principal Investigator  
Present address: Mechanical Engineering Dept, Stanford University

1 August 1988 (updated 29 August 1990).

## 1. Introduction

The main object of this work was to study, experimentally, the effects of anisotropic free-stream turbulence on heat transfer in low-speed turbulent boundary layers, with particular reference to turbomachinery applications. Typical free-stream turbulence intensities were of the order of 5 percent of the free-stream velocity - that is, typical of turbomachine blade wakes rather than the efflux from combustion chambers.

The experiments were done in three stages: first, basic measurements with isotropic free-stream turbulence, to compare with existing data; second, studies of the effect of turbulence generated by oscillating spanwise rods (a traditional method of simulating turbomachine turbulence); and third - following the abandonment of Stage Two, for reasons to be explained below - measurements of the effect of the wake of a stationary rod slightly inclined to the spanwise direction, to simulate non-radial blades. The data were intended to feed directly into the large-eddy interaction model of turbulence being developed at Purdue University. The work at Imperial College terminated when the Principal Investigator left in August 1988: fortunately this coincided with a natural break in the program, and the work continued at Stanford University in a slightly different direction. The main publications to date have been by Baskaran & Bradshaw (1989) and Baskaran, Abdellatif & Bradshaw (1989).

## 2. Equipment and Techniques

The measurements were all made in the Imperial College Aeronautics Department 30 in x 30 in closed-circuit wind tunnel, whose natural turbulence level is approximately 0.03 percent, two orders of magnitude below the level artificially generated in the present study. The test boundary layer was generated on a flat plate 8 ft in chord, with the ogive-shaped leading edge developed by Hancock to avoid leading-edge separation at rms v-component turbulence intensities up to approx. 5 percent. A trailing-edge flap was fitted to adjust the circulation around the plate to ensure symmetrical flow over the leading edge. The plate was generally similar to that used by Simonich & Bradshaw: strips of steel shim stock 1 in wide and approx. 0.001 in thick ran fore and aft, sandwiched between two sheets of plywood approx. 1/4 in thick and electrically connected in series. When the plate was heated (with an a.c. voltage of about 100V, giving a current of 13A), half the heat was transferred through the top surface and half through the bottom surface, so that the

(spatially-uniform) rate of heat transfer could be deduced directly from the electrical power input, with no correction for losses except those due to radiation. The surface temperature was measured with thin-wire thermocouples, attached to the surface with varnish which reduced the effective roughness well below the critical. The cold junctions of the thermocouples were mounted on top of plexiglass posts, projecting from the plate surface into the free stream, well to one side of the centre line on which the measurements were made. Surface shear stress was deduced either from Preston tube measurements or by fitting mean-velocity profiles to the law of the wall. Standard constant-temperature hot-wire equipment was used. More details are given by Baskaran & Bradshaw (1989).

### 3. Results

#### 3.1 First Stage - isotropic free-stream turbulence

Measurements of heat transfer and skin friction on flat plates behind conventional square-mesh grids, as used at Imperial College by Simonich (Simonich & Bradshaw 1978) and by Hancock (Hancock & Bradshaw 1989 and papers cited therein), were made as checks of techniques and of Simonich's early data, obtained before Hancock's demonstration of large effects of free-stream turbulence length scale on the skin friction for a given free-stream turbulence intensity. The results generally confirm Simonich's but show that Hancock's correlation for the combined effects of free-stream intensity and length scale does not work very well for heat transfer (i.e. Stanton number) although it is an excellent collapse of many workers' skin-friction results. The discrepancy is not merely a departure from Hancock's correlation curve: judging by the present data, Hancock's combined length-scale and intensity parameter does not provide a unique collapse of fractional changes in Stanton number as it does for fractional changes in skin-friction coefficient. The variations in Reynolds analogy factor implied by the present measurements are larger than in the work of Blair (1983).

At the end of the program a complete set of u-component spectra was measured, both throughout the boundary layer and in the free stream, to define length scale behavior in more detail (the length scale used for most of the data correlations being, for simplicity, the "dissipation length parameter" derived from estimates of dissipation deduced from free-stream turbulence decay rate).

#### 3.2 Second stage - wakes of spanwise rods

Measurements were made of the skin friction on a flat plate behind spanwise circular cylinders, either stationary or oscillating in the direction normal to the plate. Arrays of cylinders in the form of a spoked wheel, rotating about an axis in the stream direction, have been used by many workers to simulate the effect of rotor wakes on a stator, or vice versa. A mechanism to oscillate horizontal rods in the vertical direction was already available in the 30 in tunnel,

for use in studies of vortex streets behind oscillating bluff bodies. We therefore elected to use a single rod, oscillating through a sufficient amplitude in the vertical direction that the vertical velocity of translation of the wake during its interaction with the plate boundary layer was essentially constant.

Initial tests were made with the rod stationary, with its axis in the plane of the plate so that the wake met the plate leading edge symmetrically. The results showed reduced skin friction, which was unexpected in view of the increases reported by users of spoked-wheel rod arrays. The explanation was qualitatively simple, if quantitatively surprising: the effective free-stream velocity over the plate is reduced because of the reduced velocity in the wake, and evidently this outweighs the effect of the turbulence in the wake. This result is not special to the present generator and would probably be found with any stationary wake generator. Reduced skin friction was also found when the rod was oscillated vertically. However a complete row of rods or blades, rotating or not, would tend to increase skin friction. This is because skin friction depends, roughly, on (free stream velocity)<sup>2</sup>, and the increase of axial speed between the wakes, required to satisfy continuity (constant volume flow rate in the present low-speed experiment) would outweigh the effect of the velocity defect in the blade wakes.

These preliminary results rather spectacularly exposed the lack of relevance of the many previous studies of moving rod wakes, and we decided to abandon this kind of turbulence generator. The continuation of this work at Stanford University, under AFOSR grants AFOSR-86-0073 and 89-0246, uses a two-part grid to produce a turbulent wake without a mean velocity gradient, so that the effect of turbulence as such can be studied in the absence of mean-velocity variations.

### 3.3 Third stage - wake of a stationary inclined rod

An important kind of wake-blade interaction occurs when the wake is not parallel to the blade leading edge. An upstream rod IS a useful simulation of this kind of wake, if "rolled" (in the aeronautical sense of the term) at an angle to the span of the flat plate representing the downstream blade. Almost certainly, spanwise anisotropy / inhomogeneity is more important than variations normal to the plane of the blade, so this is a key configuration to study. Up to the time of closure of the Imperial College work, measurements of all mean-velocity components, all Reynolds stresses and all triple products of velocity fluctuations had been made for rod roll angles of 0, 10 and 20 deg., and for a flat-plate boundary layer in the absence of a rod (as control). A full map of the Stanton number variation over the plate surface was also obtained for all three rod angles. An obvious feature is that although spanwise variations are quite sharp, too sharp for the 3D "boundary layer" approximation to be applied, the  $W$  (spanwise) component of mean velocity and the  $uw$  and  $vw$  Reynolds stresses were fairly small, suggesting that quasi-2D "strip theory" calculations might be adequate in practice. We

have not yet used these data for test cases for calculation methods but hope that this could be done in future.

#### 4. Conclusions

Although the program at Imperial College was cut short, it yielded several useful pieces of information as well as providing data and insight for the modelling program. The simple configuration chosen to represent a turbomachine blade surface (a flat plate in low-speed flow) removed subsidiary phenomena like compressibility and pressure gradient, allowing clearer conclusions to be drawn. (i) The failure of the heat-transfer results for isotropic free-stream turbulence to collapse on the combined length-scale/intensity variable chosen by Hancock to collapse skin-friction data suggests that there are significant physical differences in the effects of free-stream turbulence on heat transfer and on skin friction (momentum transfer). (ii) The decrease in skin friction found on a flat plate in the wake of a single, stationary simulated blade exposed the misleading nature of previous workers' demonstrations of increased skin friction behind arrays of moving "blades": there is a simple explanation based on continuity arguments. (iii) Measurements on a flat plate downstream of a rod inclined in front view, simulating a non-radial blade, showed that although spanwise gradients were quite large, the spanwise mean velocity and the shear stresses with spanwise components were small: this may legitimise the use of 2-D "strip theory" methods for predicting boundary layers on such blades.

#### 5. References

Baskaran, V. and Bradshaw, P., "An experimental study into the wake-boundary layer interaction". Proceedings, 10th Australasian Fluid Mechanics Conference, Melbourne, 1989.

Baskaran, V., Abdellatif, O. and Bradshaw, P., "Effects of free-stream turbulence on turbulent boundary layers with convective heat transfer", Paper 20-1, 7th Symposium on Turbulent Shear Flows, Stanford, 1989.

Blair, M.F., "Influence of free-stream turbulence on boundary layer heat transfer and mean profile development", J. Fluids Engg vol. 105, p. 41, 1983.

Hancock, P.E. and Bradshaw, P., "Turbulence structure of a boundary layer beneath a turbulent free stream", J. Fluid Mech. vol. 205, p.45, 1989.

EXTENDED ABSTRACT

For 10th Australasian Fluid Mechanics Conference  
Dec. 1989 (P.N. Joubert Retirement Meeting)

An experimental study into the wake-boundary layer interaction

V. BASKARAN & P. BRADSHAW†

Department of Aeronautics,  
Imperial College of Science & Technology,  
London SW7 2BY, ENGLAND

### Synopsis

Mean flow and turbulence measurements were conducted in a flat plate turbulent boundary layer merging with the wake of a circular cylinder inclined in the cross-stream plane, simulating, to a first approximation, the wake of an axial turbomachine turbine blade interacting with the boundary layer over another blade downstream. Experiments were conducted for angles of inclination of the wake, with respect to the plane of the flat plate, of  $0^\circ$ ,  $10^\circ$  and  $20^\circ$ . The results demonstrate that the primary effect of the interaction is simply to reduce the skin friction due to the reduced velocity in the wake of the cylinder. The wake is bodily shifted towards the local free stream by the growing boundary layer. The turbulence of the wake, regarded as "free stream turbulence", appears to have little effect on the skin friction.

---

† Thermosci. Divn., ME Dept., Stanford University, Stanford, CA 94305.

## Introduction

This paper deals is a part of the investigation into "complex " flows at Imperial College. It is one of several papers on the interaction of a simple shear layer with another turbulent field, in this case a flat plate boundary layer interacting with the wake generated by a circular cylinder. The present work differs from earlier studies on interaction between circular cylinder wakes and boundary layers (see for example Marumo, Suzuki & Sato 1978) in that the circular cylinder was positioned well upstream of the leading edge of the flat plate on which the boundary layer grows, whereas in the earlier investigations the cylinder was held inside the turbulent boundary layer and parallel to the plate. The present flow configuration in effect idealises the flow in a turbomachine, where the wake of a blade interacts with the boundary layer over another blade downstream.

Since the leading edge and the trailing edge lines of a blade are in general not parallel, due to blade twist, the wake meets the span of the downstream blade at an angle. As a consequence, the skin friction drag and the surface heat transfer rates over the blade, and hence the overall performance of the turbomachine, is expected to be affected, in a more complicated way than if the blades were parallel. There appear to be practically no published experiments that document the above flow geometry. Therefore the purpose of the present work is to study the behaviour of a flat plate turbulent boundary layer under the influence of a circular cylinder wake meeting the leading edge at different angles. This work also has some relevance to the influence of free stream turbulence on turbulent boundary layers, with the free stream turbulence being generated by the wake of the cylinder rather than by screens or grids as in earlier work (reviewed by *e.g.* Hancock & Bradshaw 1983).

## Apparatus

The experiments were conducted in the 910 mm  $\times$  910 mm low-speed wind tunnel in the Department of Aeronautics. The experimental arrangement is shown in figure 1. The flat plate used in the present study is the same as that used by Hancock & Bradshaw (1983). A ogival-profile nose piece with sharp leading edge was used to

avoid intermittent leading-edge separation due to the random normal-component velocity fluctuations in the wake. A nominal zero pressure gradient along the stream was achieved using a flap to locate the front stagnation point at the sharp leading edge. A 16 mm diameter circular cylinder was mounted ahead of the plate spanning the test section. The leading edge of the flat plate was at 0.8 m from the circular cylinder, giving a fetch of 50 diameters for the wake to develop before it reaches the plate. The circular cylinder could be held with its axis at an angle to the span of the flat plate (figure 1). We refer to this angle as the 'wake angle' for brevity in our discussion. Experiments were performed for three wake angles, viz.  $0^\circ$ ,  $10^\circ$  and  $20^\circ$ , at a tunnel velocity of 16 m/s. The measurements included skin friction coefficients, mean velocity profiles and those turbulence quantities that appear in the transport equations for the Reynolds stress components.

## Results

Figure 2 shows the spanwise skin friction distributions at different streamwise locations for different wake angles. The distributions follow the expected trend in that the boundary layer on one half of the surface (the right half as seen looking downstream in figure 1) interacts with the wake, while the other side of the wake does not seem to affect the boundary layer since it passes under the surface. The minima of the distributions in the case of non-zero wake angle occur off the centre line. At large distances from the centre line, the distributions tend to asymptote to the two-dimensional boundary layer values.

Figure 3 shows the mean velocity profiles measured with a 1.1 mm diameter pitot tube. The profiles were measured in two planes, one along the centre line and the other -80 mm from the centre line, roughly at the position of minimum  $C_f$  (figure 2). The streamwise distance of the profiles from the leading edge in meters is as  $x = 0.152 \times$  (station number). The flat-plate profile at station 14 in the absence of the cylinder (diamond symbols in figure 3) demonstrates how the outer boundary conditions changes when the wake is present. In fact, the reduction in  $C_f$ , even at  $0^\circ$  wake angle, can be attributed to the reduced mean velocity as seen by the

undisturbed boundary layer without invoking any turbulence mechanism as such. The off-centreline profiles at small  $x$  retain the velocity minimum found in the undisturbed cylinder wake, but the profiles become monotonic at large  $x$ . Shear stress profiles are shown in figure 4. The off-centerline profiles show some remarkable differences for different wake angles due qualitatively to the change of sign of shear stress across the undisturbed cylinder wake. These profiles also demonstrate the bodily shift of wake fluid by the growing boundary layer, as indicated by the upward propagation of the maxima of the wake profile almost at the same rate as the undisturbed boundary layer thickness with downstream distance. In addition all the shear stress profiles tend to extrapolate to nearly the same value at the wall suggesting a weak influence of the turbulence in the wake on the skin friction drag.

### Conclusions

The skin friction in a turbulent boundary layer on a flat plate decreases in the presence of the wake of an upstream mounted cylinder representating an axial turbomachine blade, in contrast to the increase in  $C_f$  produced by multiple-rod grids. Evidently the primary effect is the reduction in "free stream" velocity seen by the boundary layer, as a consequence of the velocity defect in the cylinder wake: interaction between the turbulence fields of the wake and the boundary layer are less important. The details of the flow, particularly in the present case where the cylinder axis is inclined to the plane of the boundary layer, are of considerable interest.

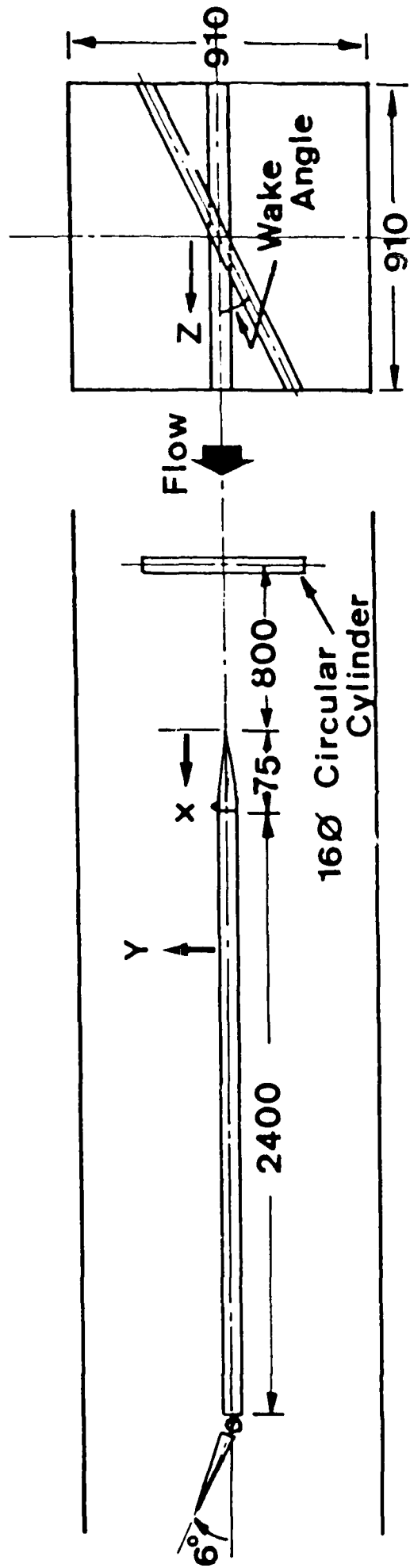
### Acknowledgements

The work was financially supported by the United States Air Force Office of Scientific Research under a sub-contract from Purdue University, monitored by Dr. S.N.B. Murthy to whom we are grateful for helpful discussions.

## References

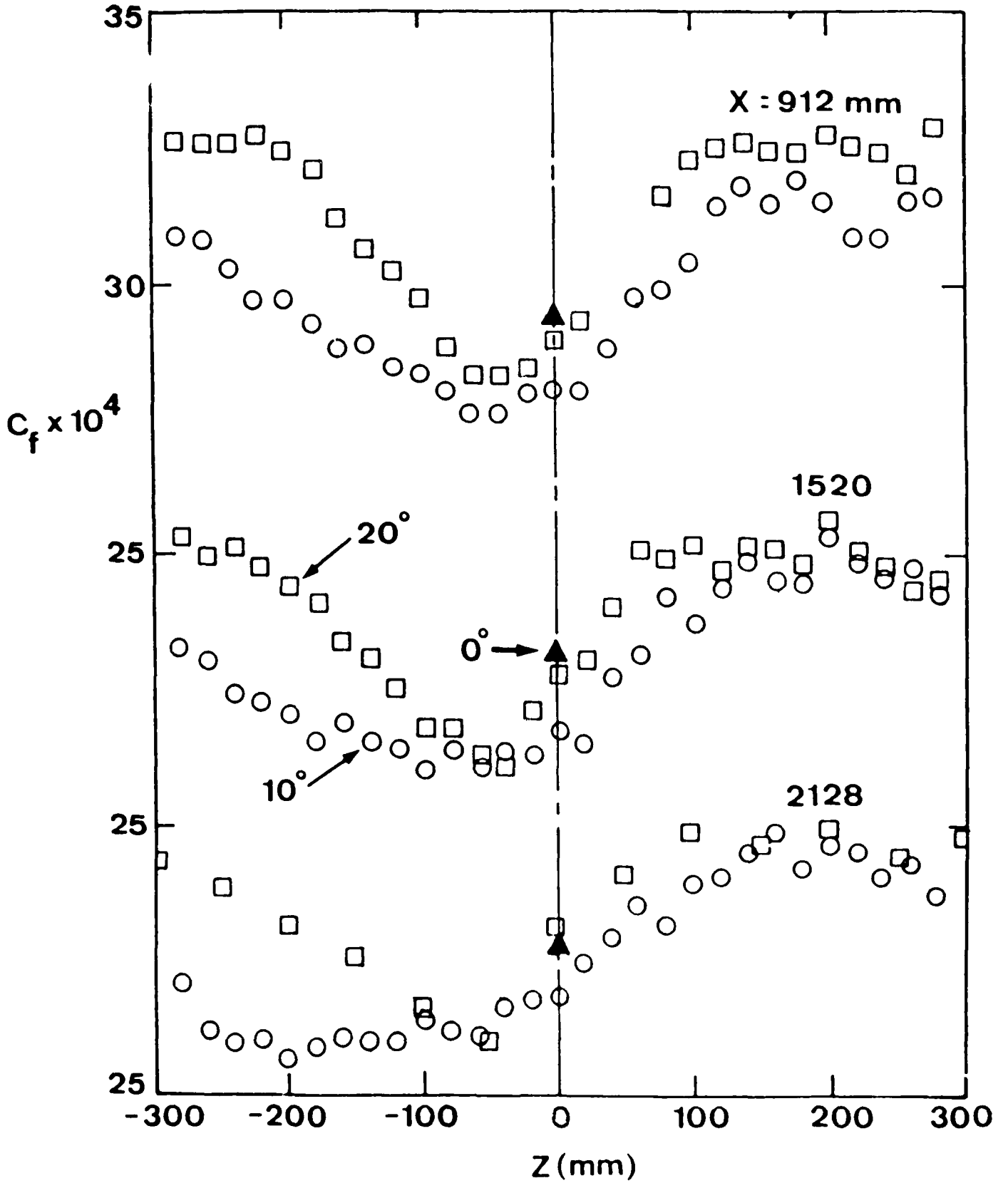
Hancock, P.E. & Bradshaw, P., The effect of free stream turbulence on turbulent boundary layers, *J. Fluids Engg.*, vol. 105, p. 244, 1983.

Marumo, E., Suzuki, K. & Sato, T., A turbulent boundary layer disturbed by a cylinder, *J. Fluid Mech.*, vol. 87, p. 121, 1978.



All dimensions in mm

Figure 1. Experimental arrangement.



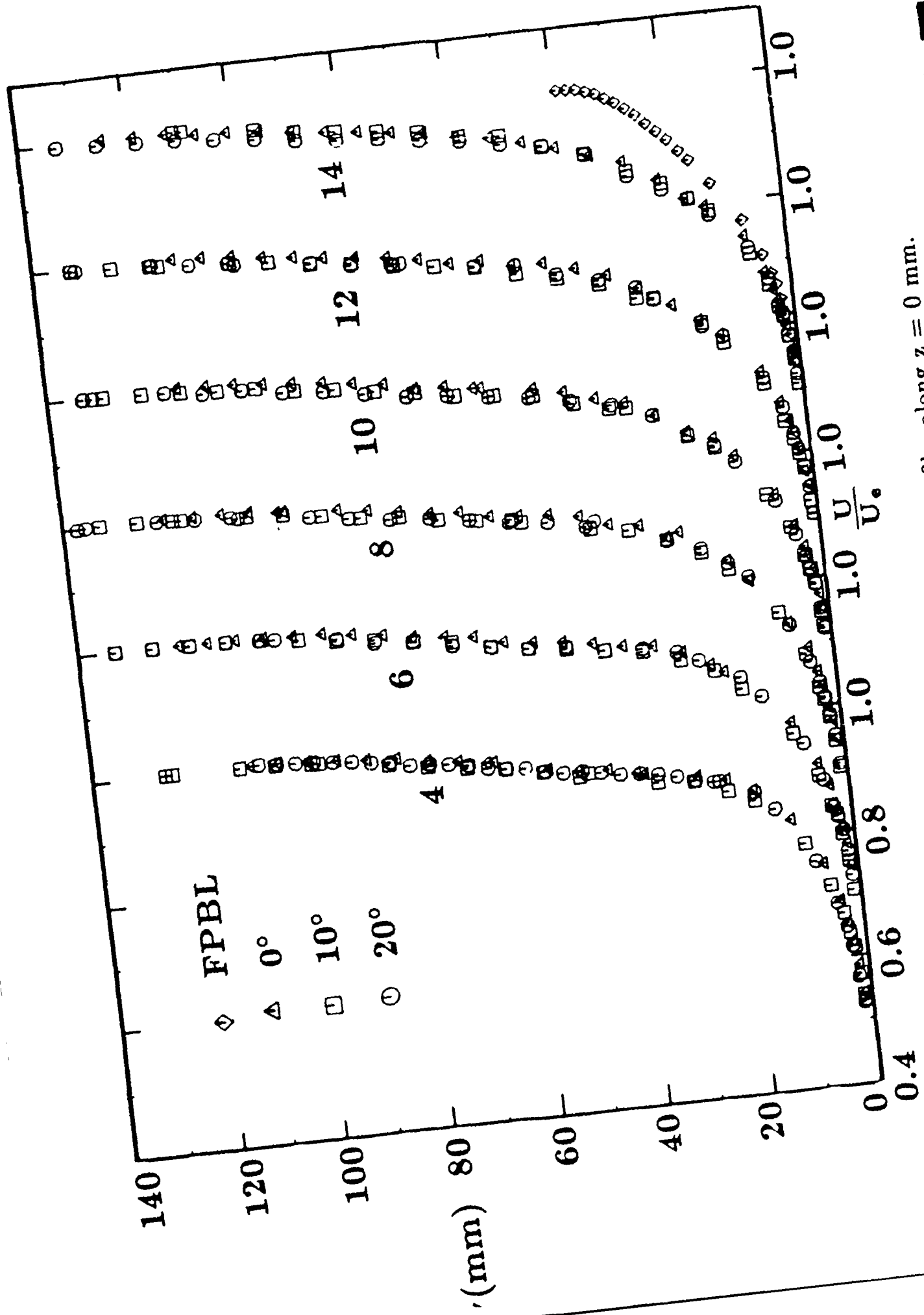


Figure 3(a). Mean velocity profiles along  $z = 0$  mm.

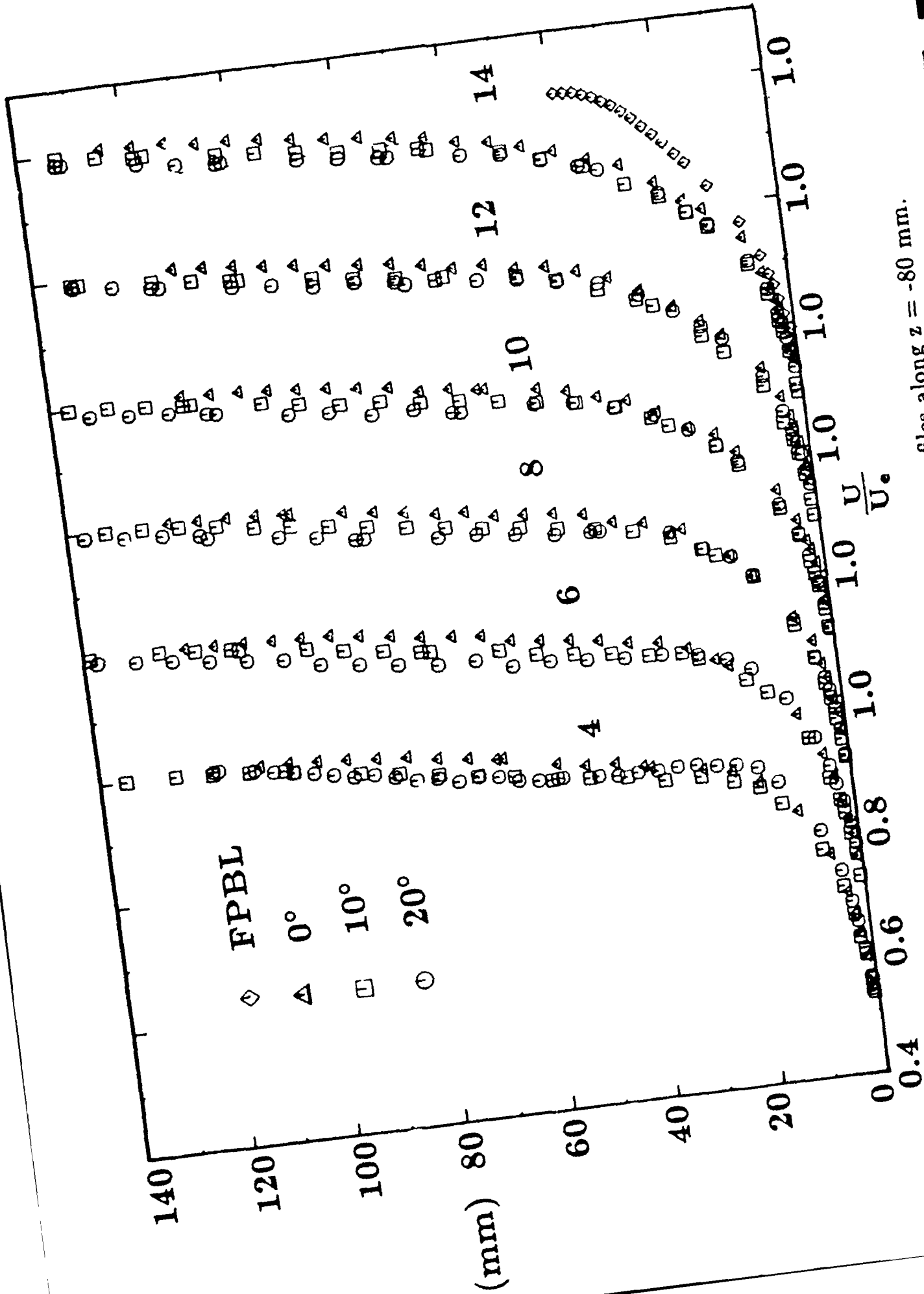


Figure 3(b). Mean velocity profiles along  $z = -80$  mm.

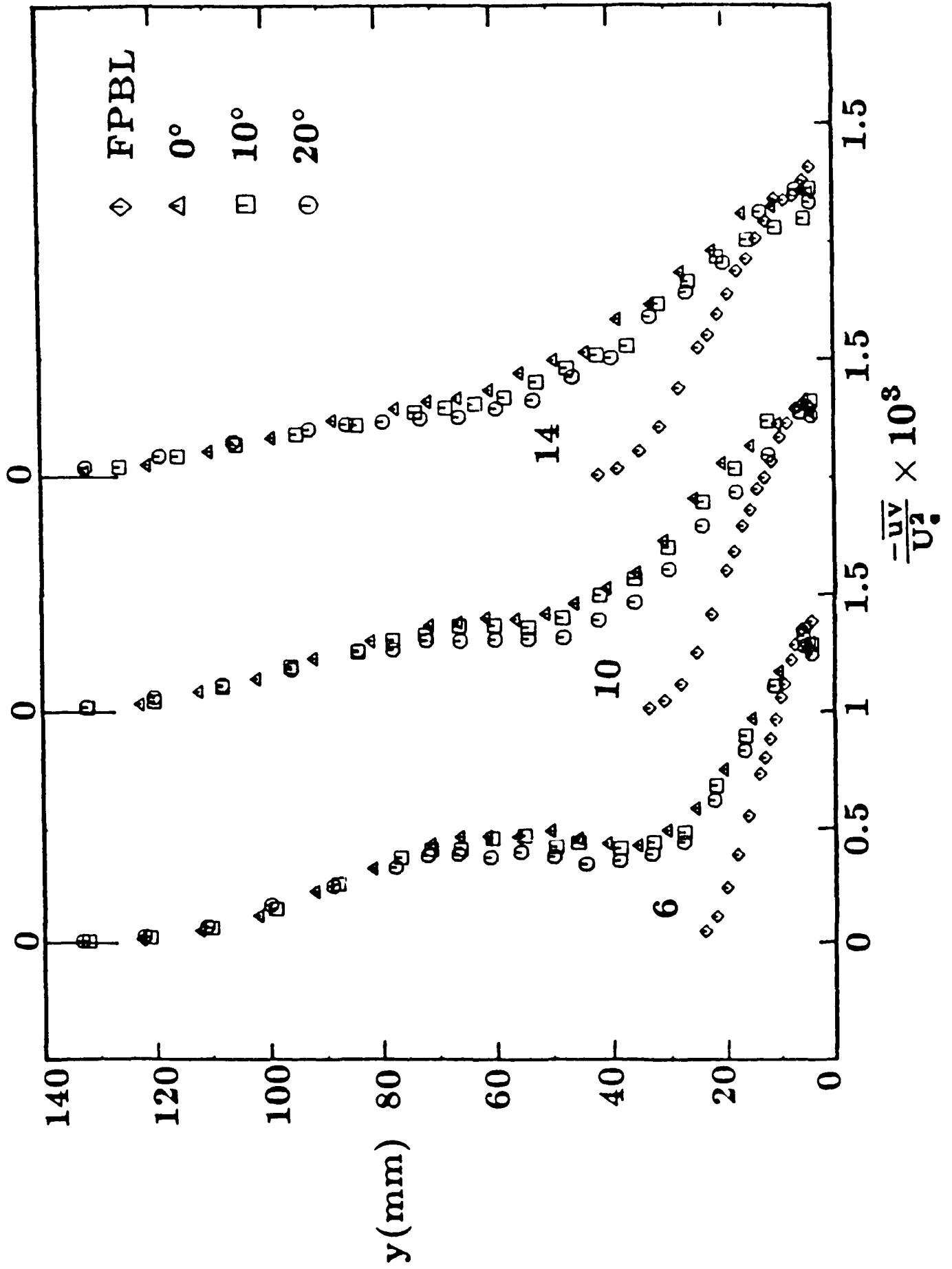


Figure 4(a). Reynolds shear stress profiles along  $z = 0$  mm.

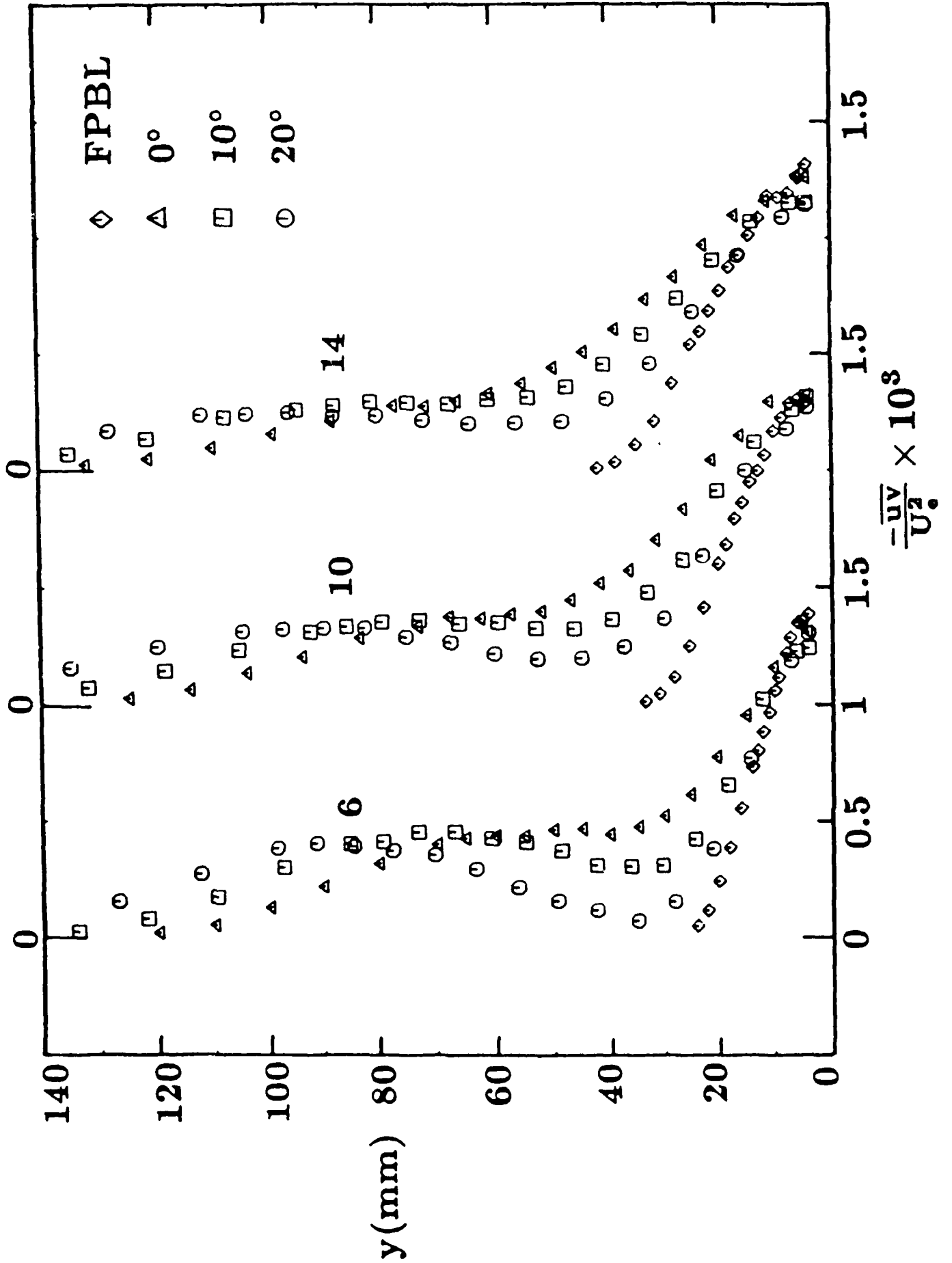


Figure 4(b). Reynolds shear stress profiles along  $z = -80$  mm.

EFFECTS OF FREE-STREAM TURBULENCE  
ON TURBULENT BOUNDARY LAYERS  
WITH CONVECTIVE HEAT TRANSFER

V. Baskaran#, O. E. Abdellatif† & P. Bradshaw‡  
Dept of Aeronautics,  
Imperial College of Science & Technology,  
London Univ.

ABSTRACT

Measurements of surface heat transfer and mean velocity have been made in a two-dimensional flat-plate turbulent boundary layer, in the presence of grid-generated free-stream turbulence. The data show that, as in the case of skin-friction coefficient, the Stanton number increases with decreasing turbulence length scale at given turbulence intensity. However, the decrease is much more rapid than in the skin-friction correlation suggested by Hancock & Bradshaw (1983). An alternative correlation is tentatively suggested. Some comments are made on previous data and on the use of arrays of rods to simulate turbomachine blade wakes.

NOMENCLATURE

$C_f$  - local skin friction coefficient,  $\tau_w/(1/2\rho U_e^2)$   
 $C_1$  - constant in equation (3)  
 $D$  - constant in equation (3)  
 $L_e$  - dissipation length scale (see equation 2)  
 $M$  - mesh size of grid  
 $n_1$  - constant in equation (3)  
 $R$  - Reynolds analogy factor,  $St/(C_f/2)$   
 $R_\theta$  - momentum-thickness Reynolds number,  $U_e\theta/\nu$   
 $St$  - Stanton number (see equation 1)  
 $T_w$  - wall temperature  
 $T_e$  - free-stream temperature  
 $U_e$  - free-stream mean velocity  
 $u_e$  - longitudinal fluctuating component of free-stream

# Aeronautical Research Labs., DSTO, Salisbury,  
Australia

† Civil Engg Dept, City Univ., London EC1

‡ Mech. Engg Dept., Stanford, CA 94305

turbulence

$x_g$  - streamwise distance from grid

$x$  - distance from plate leading edge

$y$  - normal distance from plate surface.

$\Delta C_f$  - incremental skin friction coefficient

$\delta$  - boundary layer thickness,  $y = \delta$  where  $U/U_e = 0.995$

$\Delta St$  - incremental Stanton number

Suffix o - no grid, or negligible free-stream turbulence

INTRODUCTION

The influence of free-stream turbulence (hereafter FST) on boundary layers is particularly relevant to the flow over axial-flow turbomachine blades, which suffer from the turbulence and periodic unsteadiness caused by the wakes of upstream blades, leading, for instance, to increased heat transfer to turbine blades. It is now generally recognised that the effects depend not only on the intensity of FST but also on its spectral distribution - most crudely represented by a single length scale. The present study is the start of a programme on simulation of realistic turbomachinery turbulence, now being continued at Stanford.

The simplest form of FST, which has attracted attention of many investigators, is that behind a grid, since it is easy to produce and is close to classical homogeneous isotropic turbulence. It was used at the start of the present study to check out the techniques and to improve knowledge of the effect of FST length scale on heat transfer, of which little is known even for the simplest case of a flat plate.

The next stage of the work, to be reported more fully elsewhere, was an investigation of FST produced

by the wake of a rod parallel to the test plate. Several investigators have used rotating or translating arrays of rods to simulate turbomachine blade rows. We started by studying the effect of a single, stationary rod, and found that it decreased the skin friction on the flat plate behind it: quite simply, the effect of reduced mean velocity in the rod wake was larger than that of the wake turbulence! Because skin friction varies roughly as (free-stream velocity)<sup>2</sup>, time-average skin friction for a given mass-flow rate is increased by a translating array of rods, simply because of the increased free-stream velocity between the rod wakes: heat transfer, which is to a first approximation directly proportional to free-stream velocity, would be comparatively little affected. This fact about rod arrays does not seem to have been noticed by previous users. Work on more meaningful simulation of turbomachine turbulence – as distinct from periodic unsteadiness – is in progress.

Several attempts have been made to correlate changes in skin friction coefficient  $C_f$  and Stanton number  $St$  with FST produced by grids. Simonich & Bradshaw (1978) suggested that the increase in  $C_f$  or  $St$  is directly proportional to the rms longitudinal turbulence intensity, with a five percent increase in  $St$  for each one percent of rms turbulence (compared to about 3 percent for  $C_f$ ). They ignored any effects of turbulence length scale. Later, Hancock & Bradshaw (1983: hereafter cited as HB) measured the effects of grid turbulence with a wide range of length scales, and put forward a more general form of correlation for the fractional change in skin-friction coefficient with both velocity and length scales, as a function of the empirical variable,  $(\sqrt{u_c^2}/U_c)/(L_c/\delta + 2)$ . The correlation is strongly non-linear in rms intensity  $\sqrt{u_c^2}$ , and the effects of length scale are large, at least in the range of the experiments,  $1.5 < L_c/\delta < 6$ . Blair (1983) and Castro (1984) have extended the correlation to low Reynolds numbers, where viscous effects on the outer layer interact with those of FST.

Blair found good agreement between his Stanton-number measurements in grid turbulence and the HB correlation with the ordinate multiplied by 1.3, for fractional increments in  $St$  up to about 0.2. For higher turbulence levels, the HB correlation predicts that the increase in  $C_f$  becomes slower, but Maciejewski &

Moffat (1988) and MacMullin, Elrod & Rivir (1988) have found that  $St$  increases far more than  $C_f$  at high levels of non-isotropic FST, with roughly a factor of four increase in  $St$  at 40 percent turbulence, so that Blair's conclusion is evidently not generally valid. (Maciejewski & Moffat's data do not collapse on any combination of length scale and intensity.) In 1953 Sugawara, Sato, Komatsu & Osaka (1988) found that, in grid turbulence, the factor of increase of  $St$  tended to an almost constant value of about 1.55 at rms intensities of 7 or 8 percent (the limit of their data), while Šlančiauskas & Pedišius (1978) found an almost constant value of 1.4 for 10 to 17 percent turbulence. The latter authors found that the factor of increase of  $St$  was about 1.7 times the factor of increase in  $C_f$  for all FST values, but this cannot be directly compared with Blair's 1.3 because Šlančiauskas & Pedišius ignored length-scale effects. The situation is confused, especially as regards length-scale effects.

We have repeated the experiments of Simonich & Bradshaw (1978) over about the same range of intensities as used by Blair, but over the wider range of length scales used by HB. Our  $C_f$  distributions agree with the HB correlation but the Stanton-number distributions do not, even if the constant of proportionality is adjusted: the experiment was cut short by the authors' departure from Imperial College but the data are offered as a partial insight into length-scale effects over a wider range than previous work. A tentative modification to the  $C_f$  correlation is suggested to correlate  $St$ .

## APPARATUS AND TECHNIQUES

The measurements were made in the 910 mm × 910 mm closed-circuit wind tunnel used by Simonich & Bradshaw (1978) and Hancock & Bradshaw (1983). The flat plate (figure 1) is also that used by Simonich & Bradshaw. An ogival leading edge was used to avoid intermittent leading-edge separation due to normal-component velocity fluctuations. Nominally zero pres-



Figure 1. Experimental Arrangement.

sure gradient along the rest of the plate was achieved by using a trailing-edge flap. A 1.2 mm trip wire was attached 80mm from the leading edge. The biplane grids used by HB, with square bars at pitches of 38 mm, 76 mm and 152 mm were inserted at the start of the working section. The leading edge of the flat plate was 2.09 m from the grid. All measurements were made at a free-stream velocity of 21 m/s, as in the earlier studies at Imperial College. At this speed the turbulence level in the empty working section was found to be approximately 0.03 percent.

The resistive element used to heat the plate consisted of 30 stainless steel strips, 0.05 mm thick and 25 mm wide, connected in series and sandwiched between two 6 mm thick plywood boards 2.4 m long, so that when steady conditions were reached the heat transfer from each surface of the plate was half the electrical power input and direct measurement was not needed. The cold resistance of the element was typically 8Ω. In the present study, a power input of 1.3kW (13A and 100V) was used: Simonich and Bradshaw used only 450W. The mean temperature difference between the surface and the free stream was in the range of 4–7°C, and was measured using Cromel-Alumel thermocouples imbedded in the surface of the plate, with the cold junctions mounted in the free stream on the tops of Perspex masts. The thermocouples were calibrated using ice blocks and hair driers, and the constant of calibration was found to be typically 40μV/°C.

The Stanton number was deduced as

$$St = \frac{W/A}{\rho c_p (T_w - T_e) U_e} \quad (1)$$

where  $W$  is the electrical power input and  $A$  is the total area of the plate. Radiation losses were estimated to be about 10 to 15 percent of the convective transfer.

Mean velocity profiles were measured on-line to a BBC Model B microcomputer, using a 1.1 mm pitot tube. Mean temperature profiles were measured with a thermocouple probe, which proved to suffer from excessive wall effects, so the results are not given here. Local  $C_f$  was deduced by fitting the mean velocity profiles to the logarithmic law of the wall with constants 0.41 and 5.2, as the law of the wall was found to be unaffected by FST in the range of intensities used by HB.

The longitudinal component of the turbulent intensity behind various grids was measured along the centre-line of the working section in the absence of the plate, using a normal hot-wire and a Melbourne University type constant-temperature anemometer. The length scale of the FST was derived from the decay of the longitudinal component of the turbulent intensity, using Taylor's hypothesis for frozen turbulence, as

$$L_e = - \frac{(\overline{u_e^2})^{3/2}}{U_e (d\overline{u_e^2}/dx)} \quad (2)$$

If the turbulence were isotropic, with turbulent kinetic energy  $k$  equal to  $3\overline{u_e^2}/2$ , this length scale would be  $\sqrt{2/3}$  times the true dissipation length scale  $k^{3/2}/\epsilon$ .

### RESULTS

Figure 2 shows the variation of the longitudinal turbulent intensity for each grid, with the limited data of Simonich & Bradshaw (1978). Note that the maximum turbulence level that the plate encounters is

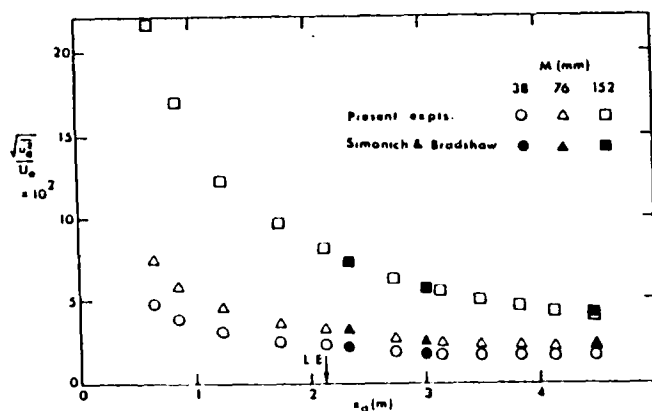


Figure 2. Streamwise distributions of the longitudinal turbulent intensity behind grids.

about 8 percent. According to Comte-Bellot & Corrsin (1966), the decay of the longitudinal turbulent intensity can be expressed in the form

$$\left(\frac{\overline{u_e^2}}{U_e^2}\right) = C_1^2 \left(\frac{x_g}{M} - D\right)^{-n_1} \quad (3)$$

where  $C_1$ ,  $D$  and  $n_1$  are constants for a given grid of mesh size,  $M$ . Best-fit values for the present data are given in Table 1.

$M(\text{mm})$	38	76	152
$C_1^2$	0.0659	0.0476	0.07
$D$	4.0	4.81	3.63
$n_1$	1.25	1.25	1.25

Table 1.

The streamwise distributions of the length scale  $L_e$  derived from equation 2 are shown in figure 3, non-dimensionalised using the local boundary layer thickness. The length scale varies from 1.5 to 6 times the local boundary layer thickness, as in the HB experiments. Note that  $L_e$  increases with  $x$ , but more slowly than  $\delta$ .

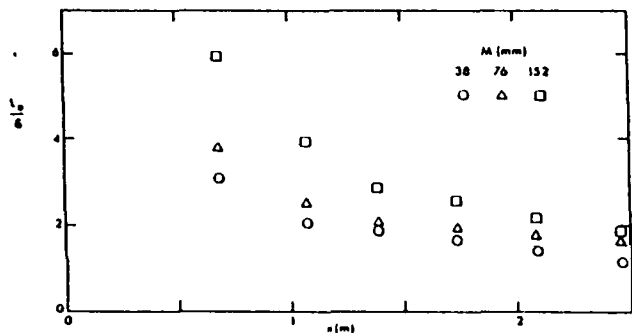


Figure 3. Streamwise distributions of non-dimensional dissipation length scale behind grids.

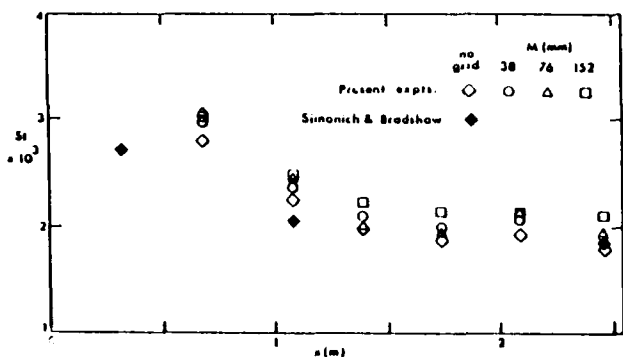


Figure 4. Streamwise distributions of Stanton number in the heated flat plate turbulent boundary layer.

The streamwise distributions of  $St$  for the different grids are shown in figure 4, which includes the distributions obtained by Simonich & Bradshaw and in the present study without a grid. The initial difference in the  $St$  distribution between the two cases is due to the adverse pressure gradient aft of the leading edge, which was stronger in Simonich & Bradshaw's work.

The  $C_f$  and  $St$  distributions are plotted against the momentum thickness Reynolds number in figures 5 and 6, as the effects of FST are best evaluated at fixed  $R_\theta$ : nearly all the results lie above the upper limit of significant interaction between the effects of FST and of low Reynolds number ( $R_\theta \approx 2000$  according to Castro). The present  $C_f$  data corresponding to negligible FST (no grid) are in good agreement with the general  $C_f - R_\theta$  correlation proposed by Coles (1962) and with the earlier Imperial College data. The no-grid Stanton number at  $R_\theta = 5000$  is about 4 percent higher than the correlation of Kays & Crawford (1980).

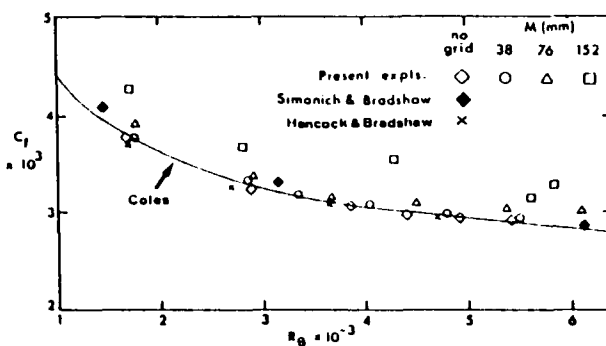


Figure 5. Skin friction coefficient versus momentum thickness Reynolds number.

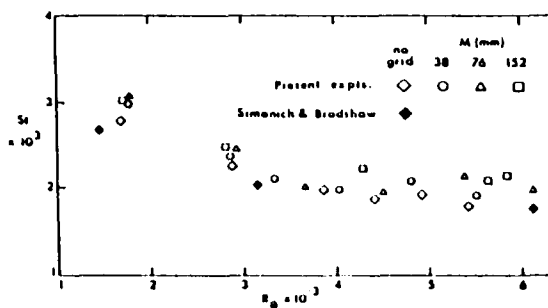


Figure 6. Stanton number versus momentum thickness Reynolds number.

Figure 7 shows the  $C_f$  correlation of HB with the results of the present and previous Imperial College studies. The agreement is generally within  $\pm 2$  percent of  $C_f$ . The fractional changes in  $St$  are plotted against the empirical parameter of HB in figure 8, together with the limited data of Simonich & Bradshaw. Our measured values of  $St/St_0$ , as well as those of Simonich & Bradshaw, lie well above the  $C_f$  correlation curve of HB. It follows that the Reynolds analogy factor  $St/(C_f/2)$  is affected by FST. (The Reynolds analogy factor is plotted against  $R_\theta$  in figure 9 as an illustration of this but the grid-to-grid changes

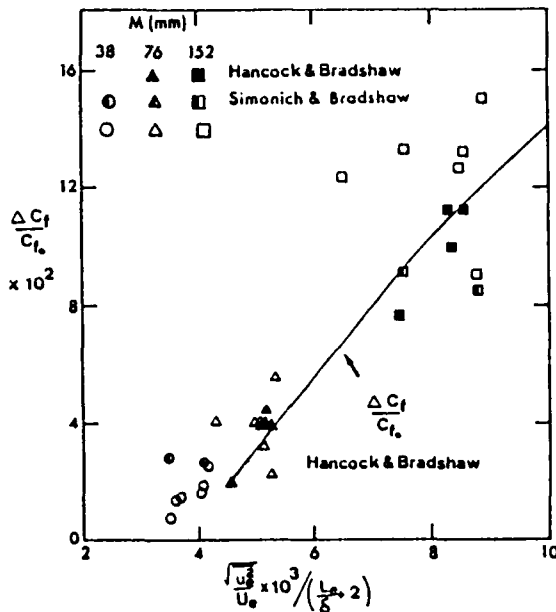


Figure 7. Fractional changes in skin friction coefficient versus  $\frac{\sqrt{u_e^2}}{U_e} \cdot 10^3 / (\frac{L_e}{\delta} - 2)$ .

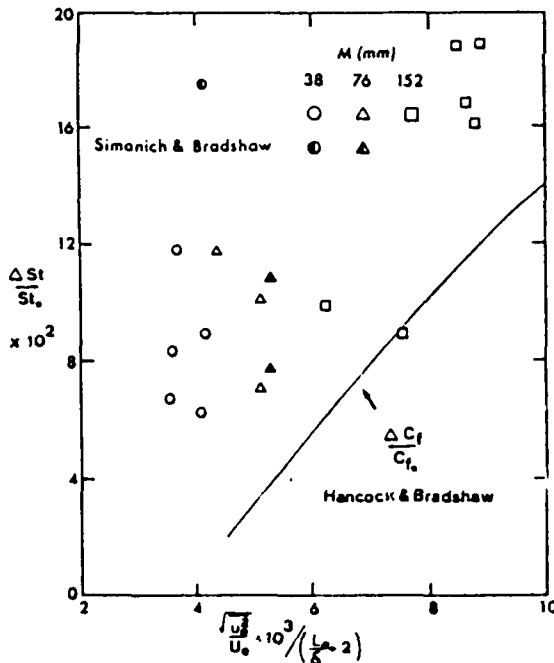


Figure 8. Fractional changes in Stanton number versus  $\frac{\sqrt{u_e^2}}{U_e} \cdot 10^3 / (\frac{L_e}{\delta} - 2)$ .

in these axes are not expected to be simple.) Exact analogy ( $St/(C_f/2) = 1$ ) requires molecular and turbulent Prandtl numbers to be unity, but in the outer layer, where the main effects of FST are felt, the tur-

bulent Prandtl number in the absence of FST is about 0.7. With no grid, the Reynolds analogy factor  $R$  at  $Re > 3000$  is about 1.22, but it increases to roughly 1.3 at the higher turbulence levels. At lower Reynolds number the change in  $St/(C_f/2)$  is larger but the fractional change in  $St/(C_f/2) - 1$  is roughly the same. Blair correlated his data as  $R = 1.18 + 1.3(\sqrt{u_e^2}/U_e)$  for all length scales, a smaller variation than in the present data. It can be shown easily that

$$\Delta St/St_o = (R/R_o)[1 + (\Delta C_f/C_{fo})] - 1 \quad (4)$$

where  $R$  and  $R_o$  are the Reynolds analogy factors corresponding to finite FST level and negligible FST: correlations of analogy factor rather than  $St$  may be convenient for designers, but at present it seems most straightforward to modify the HB correlation for  $C_f$  and apply it to  $St$ .

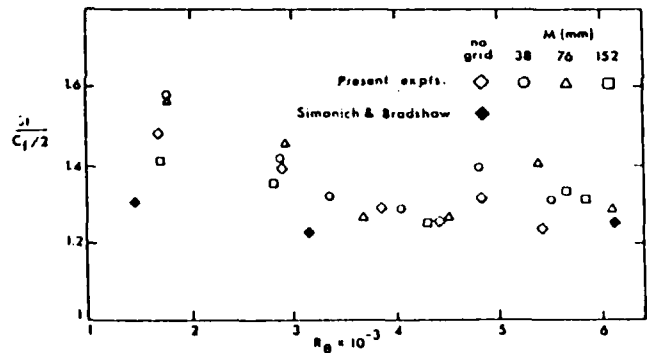


Figure 9. Reynolds analogy factor versus momentum thickness Reynolds number.

If the data in figure 8 are reliable they imply that HB's empirical parameter for  $C_f$  underestimates the effect of FST length scale on  $St$ . The denominator would have to be changed to about  $(L_e/\delta - 1)$  to bring the 152 mm grid results close to the others, and this is clearly unacceptable as a general correlation since  $L_e/\delta = 1$  is in the range of practical interest. A fairly good collapse is obtained by changing the denominator to  $(L_e/\delta + 2)^3$ , but of course the correlation function is no longer a factored form of Hancock & Bradshaw's.

### CONCLUSIONS

Skin friction coefficients and Stanton numbers were measured in a flat plate boundary layer beneath grid-

generated free stream turbulence, with a maximum rms intensity of 8 percent of the free stream velocity and a maximum length scale of 6 times the local boundary layer thickness. The increase in skin friction coefficient agrees well with the correlation curve based on the variable,  $\sqrt{u_2^2}/U_c/(L_c/\delta+2)$ , proposed by Hancock & Bradshaw (1983). Stanton number increases do not seem to follow the proposed skin friction correlation or any simple multiple of it, indicating that the Reynolds analogy factor is changing significantly - more than in the work of Blair (1983). A change in the above empirical variable to improve Stanton number predictions is tentatively suggested.

The wake of a spanwise rod mounted ahead of the test plate to simulate turbomachine blade wakes produced a *reduction* in skin friction, calling into question the interpretation of published results from moving rod arrays.

#### ACKNOWLEDGEMENTS

The work was financially supported by the U.S. Air Force Office of Scientific Research under a sub-contract from Purdue University. We are grateful to Dr. S.N.B. Murthy and Dr R.B. Rivir for encouragement and helpful discussions.

#### REFERENCES

- BLAIR, M.F. 1983 Influence of free-stream turbulence on boundary layer heat transfer and mean profile development. *J. Heat Transf.* **105**, 41.
- CASTRO, I.P. 1984 Effects of free stream turbulence on low Reynolds number turbulent boundary layers. *J. Fluids Engg* **106**, 298.

COLES, D.E. 1962 The turbulent boundary layer in a compressible fluid. *RAND Corp. Rept.* R-403-PR.

COMTE-BELLOT, G. & CORRISIN, S. 1966 The use of a contraction to improve isotropy of grid generated turbulence. *J. Fluid Mech.* **25**, 657.

HANCOCK, P.E. & BRADSHAW, P. 1983 The effect of free-stream turbulence on turbulent boundary layers. *J. Fluids Engg.* **105**, 244.

KAYS, W.M. & CRAWFORD, M.E. 1980 *Convective Heat and Mass Transfer*. McGraw-Hill, New York.

MACIEJEWSKI, P.K. & MOFFAT, R.J. 1988 The effect of high free-stream turbulence on heat transfer in turbulent boundary layers. Presented at Zaric Memorial Seminar on Near-Wall Turbulence, Dubrovnik.

MacMULLIN, R., ELROD, W. & RIVIR, R.B. 1988 Effects of free stream turbulence from a circular wall jet on a flat plate heat transfer and boundary layer flow. ASME paper 88-IGT-183, *J. Turbomach.* **111**, 1 (1989).

SIMONICH, J.C. & BRADSHAW, P. 1978 Effect of free-stream turbulence on heat transfer through a turbulent boundary layer. *J. Heat Transf.* **100**, 371.

ŠLANČIAUSKAS, A. & PEDIŠIUS, A. 1978 Effect of free-stream turbulence on the heat transfer in the turbulent boundary layer. 6th International Heat Transfer Conf., Toronto, **2**, 513.

SUGAWARA, S., SATO, T., KOMATSU, H. & OSAKA, H. 1988 *Int J. Heat Mass Transf.* **31**, 5 (translation of *Trans. Jap. Soc. Mech. Engrs* **19**, 18, 1953).